Metabolic Engineering 75 (2023) 153–169

Contents lists available at ScienceDirect

Metabolic Engineering

journal homepage: www.elsevier.com/locate/meteng

Systems metabolic engineering upgrades *Corynebacterium glutamicum* to high-efficiency *cis, cis*-muconic acid production from lignin-based aromatics

Fabia Weiland, Nadja Barton, Michael Kohlstedt, Judith Becker, Christoph Wittmann *

Institute of Systems Biotechnology, Saarland University, Saarbrücken, Germany

ARTICLE INFO

Keywords:
Corynebacterium glutamicum
Bio-based
cis
cis-muconic acid
Vanillin
Vanillate
Vanillyl alcohol
AroY
FudC
Softwood
Lignin
Hydroxycinnamates
Ferulate
p-Coumarate
Caffeate
p-Hydroxybenzoate
Protocatechuate
p-Hydroxybenzaldehyde
Protocatechualdehyde
Aromatic compounds
Alkaline oxidation

ABSTRACT

Lignin displays a highly challenging renewable. To date, massive amounts of lignin, generated in lignocellulosic processing facilities, are for the most part merely burned due to lacking value-added alternatives. Aromatic lignin monomers of recognized relevance are in particular vanillin, and to a lesser extent vanillate, because they are accessible at high yield from softwood-lignin using industrially operated alkaline oxidative depolymerization. Here, we metabolically engineered *C. glutamicum* towards *cis, cis*-muconate (MA) production from these key aromatics. Starting from the previously created catechol-based producer *C. glutamicum* MA-2, systems metabolic engineering first discovered an unspecific aromatic aldehyde reductase that formed aromatic alcohols from vanillin, protocatechualdehyde, and *p*- hydroxybenzaldehyde, and was responsible for the conversion up to 57% of vanillin into vanillyl alcohol. The alcohol was not re-consumed by the microbe later, posing a strong drawback on the producer. The identification and subsequent elimination of the encoding *fudC* gene completely abolished vanillyl alcohol formation. Second, the initially weak flux through the native vanillin and vanillate metabolism was enhanced up to 2.9-fold by implementing synthetic pathway modules. Third, the most efficient protocatechuate decarboxylase AroY for conversion of the midstream pathway intermediate protocatechuate into catechol was identified out of several variants in native and codon optimized form and expressed together with the respective helper proteins. Fourth, the streamlined modules were all genomically combined which yielded the final strain MA-9. MA-9 produced bio-based MA from vanillin, vanillate, and seven structurally related aromatics at maximum selectivity. In addition, MA production from softwood-based vanillin, obtained through alkaline depolymerization, was demonstrated.

1. Introduction

The aromatic heteropolymer lignin is an important structural compound of lignocellulosic biomass and makes up 15–30% of its dry weight (Bugg et al., 2011). Characterized by a high heterogeneity and versatility (del Río et al., 2020), lignin is, also, the only renewable source for aromatic compounds (Tuck et al., 2012), spurring on valorization efforts, despite its challenging nature (Abu-Omar et al., 2021). Lignocellulosic processing facilities generate massive amounts of technical lignins during biomass fractionation (Kienberger et al., 2021), whereby the pulp and paper industry alone annually generates 50 Mt of Kraft lignin (Bruijnincx et al., 2015). Additionally, agricultural residues display a recurring potential source of lignins, contributing approximately 180 Mt of lignin on top (Gonçalves et al., 2020).

Due to the lack of more value-adding alternatives, technical lignins are majorly burned (Abdelaziz et al., 2016) (i) unfavorably contributing to global warming, (ii) limiting the economic efficiency of lignocellulosic biorefineries, overall showing that the current underutilization of large volumes of this global renewable resource is highly unfavorable (Becker and Wittmann, 2019). It goes without saying that this situation raises lignin valorization one of the most urgent but also most enabling topics in bioeconomy (Abu-Omar et al., 2021). Over the recent years, selected soil microbes, naturally capable to depolymerize lignin and degrade aromatic compounds (Brink et al., 2019; Tian et al., 2014), have proven valuable for lignin-based value-adding applications (Becker and Wittmann, 2019; Bugg et al., 2021). The industrial flagship among

* Corresponding author.
E-mail address: christoph.wittmann@uni-saarland.de (C. Wittmann).

https://doi.org/10.1016/j.ymben.2022.12.005
Received 13 October 2022; Received in revised form 14 December 2022; Accepted 17 December 2022
Available online 20 December 2022

lignin-based chemicals, derived through engineered microbes, is *cis, cis*-muconate (MA) (Weiland et al., 2022), well reflected by a world market of $ 22 billion (Sonoki et al., 2014). Notably, MA itself is a suitable monomer for polymers (Rorrer et al., 2016) and, furthermore, serves as a precursor for other commercial chemicals, including adipic acid and terephthalic acid (Khalil et al., 2020; Xie et al., 2014), recently enabling bio-nylon (Kohlstedt et al., 2018) and bio-PET (Kohlstedt et al., 2022) from lignin. Notably, based on its high potential to be converted into a broad range of different chemicals, MA was also recently labelled as a "bio-privileged molecule" (Shanks and Broadbelt, 2019; X. Zhou et al., 2019b).

From a metabolic perspective, MA is an intermediate in the catabolic β-ketoadipate pathway (Barton et al., 2018; Becker et al., 2018a; Cai et al., 2020; Kohlstedt et al., 2018; Salvachúa et al., 2018; Shinoda et al., 2019). The natural setup of the pathway allows MA production only *via* catechol as a central intermediate. However, many lignin-derived aromatics are catabolized *via* protocatechuate (Vardon et al., 2015), disconnected from catechol. Bridging this gap by introducing protocatechuate decarboxylase-encoding genes, allows the connection of both branches at the level of their central intermediates and enables the valorization of hydroxycinnamates such as ferulate and *p*-coumarate (Vardon et al., 2015).

In this work, we upgraded *C. glutamicum*, well-known for its leading role in the sugar-based bioindustry (Becker et al., 2018b; Wolf et al., 2021), to produce MA from two relevant lignin-based aromatic monomers, namely vanillin and vanillate (Bjørsvik and Liguori, 2002; Fache et al., 2016). Different to e. g., hydroxycinnamates, also named phenylpropanoids (Kallscheuer et al., 2016), from agricultural residues (Elmore et al., 2021; Rodriguez et al., 2017; Salvachúa et al., 2018) or phenolics from hydrothermal lignin-hydrolysates (Barton et al., 2018; Becker et al., 2018a; Kohlstedt et al., 2018), the two aromatics have not been extensively explored to date as a substrate in bacterial lignin valorization strategies (Suzuki et al., 2021; Zhou et al., 2022). However, vanillin, and to a lesser extent vanillate, are accessible at high yield through catalytic alkaline oxidation of softwood lignin (Fache et al., 2016; Hirano et al., 2022; Wouter Schutyser et al., 2018a; Silva et al., 2009; Vu et al., 2021). The process is established since several decades at industrial scale (Pacek et al., 2013) to produce approximately 3,000 tons of the flavoring agent vanillin (Fache et al., 2016). Obviously, this route withdraws only a small stream, so that, still, 400 kg of lignin remain per 1000 kg of softwood lignin (Rødsrud, 2018), suggesting a huge valorization potential.

Starting from *C. glutamicum* MA-2, recently created to produce MA from catechol (Becker et al., 2018a), we used several rounds of systems metabolic engineering to (i) identify and eliminate an unspecific aromatic aldehyde reductase that caused the accumulation of undesired aromatic alcohols as dead-end products, (ii) balance the natural oxidative and reductive pathways for vanillin metabolization, (iii) tailor vanillate uptake, (iv) fine-tune the coupling of the flux from the protocatechuate to the catechol node by a most efficient protocatechuate decarboxylase along with the associated helper proteins, and (v) combine all created synthetic pathways modules in one cell factory. The finally obtained advanced strain *C. glutamicum* MA-9 efficiently produced MA from lignin-derived vanillin and vanillate, and, additionally, seven other lignin-associated aromatics were converted into MA at maximum selectivity.

2. Materials and methods

2.1. Microorganisms and plasmids

C. glutamicum ATCC 13032 (DSM 20300) was obtained from the German Collection of Microorganisms and Cell Cultures (DSMZ, Braunschweig, Germany). The basic MA-producer *C. glutamicum* MA-2, featured by the deletion of muconate cycloisomerase (*catB,* NCgl2318) and the overexpression of catechol-1,2-dioxygenase (*catA*, NCgl2319) was taken from previous work (Becker et al., 2018a). *E. coli* DH10B (Life GmbH, Darmstadt, Germany) and NM522 (Invitrogen, Carlsbad, CA, USA) were used for plasmid amplification. The latter co-expressed pTC to add the *C. glutamicum*-specific DNA-methylation pattern to plasmid DNA (Kind et al., 2010). All strains were preserved as frozen cryo-stocks in 30% glycerol at -80°C. For genome-based deletion, as well as an integration or overexpression of genes, integrative transformation vectors, based on pClik int *sacB*, were used (Becker et al., 2005; Kind et al., 2010). All strains and plasmids used in this study are listed in Table 1.

2.2. Genetic engineering

For the design of strains, plasmids, and primers, the software SnapGene was used (GSL Biotech LLC, Insightful Science, Chicago, IL, USA). For plasmid construction, the integrative vector pClik int *sacB* was linearized *via* restriction with *Bam*HI (FastDigest, Thermo Fisher Scientific, Waltham, MA, USA), under supplementation of alkaline phosphatase (FastAP Thermosensitive Alkaline Phosphatase, Thermo Fisher Scientific). All required DNA-fragments were amplified by PCR (2 x Phusion High-Fidelity PCR Master Mix with GC Buffer, Thermo Fisher Scientific) using construct-dependent, sequence-specific primers (Table S1, Supplementary File 1), purified (Wizard SV Gel, PCR Clean-Up System, Promega, Mannheim, Germany), and subsequently assembled with the linearized vector (Rohles et al., 2016). Heterologous genes for expression in *C. glutamicum* were synthetized, based on digital sequence information, either in native or codon-optimized manner (BioCat, Heidelberg, Germany). The latter adapted the codon usage to the preference of *C. glutamicum* (http://www.kazusa.or.jp) (Table S2, Supplementary File 1). Protein identification for genetic engineering used the Basic Local Alignment Search Tool (Altschul et al., 2005) (BLASTP, https://blast.ncbi.nlm.nih.gov/Blast.cgi) with amino acid sequences of identified proteins as input (Tables S3–S5, Supplementary File 1) (Rohles et al., 2022). The relative adaptiveness of introduced heterologous gene sequences to the codon usage of *C. glutamicum* and to that of the donor strains, respectively, was investigated by the Graphical Codon Usage Analyzer (https://gcua.schoedl.de/) (Rohles et al., 2022). For amplification, plasmids were first transformed into *E. coli* DH10B, followed by an isolation from correct clones (QIAprep Spin Miniprep Kit, Qiagen, Hilden, Germany). After transformation into *E. coli* NM522+pTC for amplification and methylation, plasmid DNA was isolated and transformed into *C. glutamicum*. Transformation of *E. coli* by heat-shock, transformation of *C. glutamicum* by electroporation, as well as the subsequent generation of defined mutants was carried out as described in earlier studies (Becker et al., 2010; Kind et al., 2010; Rohles et al., 2022). Plasmids and strains were validated by PCR (Table S1, Supplementary File 1) and sequencing (Azenta Life Sciences, Genewiz Germany, Leipzig, Germany).

2.3. Media

C. glutamicum and *E. coli* were routinely grown in complex medium (37 g L^{-1} brain heart infusion, BHI, Becton Dickinson, Franklin Lakes, NJ, USA). If appropriate, the complex medium was supplemented with 20 g L^{-1} BD Difco agar (Becton Dickinson) for solidification, and with different antibiotics (50 μg mL^{-1} kanamycin, 12.5 μg mL^{-1} tetracycline) for plasmid maintenance in *E. coli*, respectively. For the cultivation of *C. glutamicum*, a minimal medium was used which contained per liter: 11 g of glucose monohydrate, 34.8 g of K_2HPO_4, 27.2 g of KH_2PO_4, 15 g of $(NH_4)_2SO_4$, 1 g of NaCl, 0.2 g of $MgSO_4*7H_2O$, 0.055 g of $CaCl_2$, 2 mg of $FeCl_3*6H_2O$, 2 mg of $MnSO_4*H2O$, 0.5 mg of $ZnSo_4*H_2O$, 0.2 mg of $CuCl_2*2H_2O$, 0.2 mg of $Na_2B_4O_7*10H_2O$, 0.1 mg of $(NH_4)_6Mo_7O_{24}*4H_2O$, 20 mg of $FeSO_4*7H_2O$, 1 mg of thiamin-HCl, 1 mg of Ca-pantothenate, 0.5 mg of biotin, and 30 mg of 3,4-dihydroxybenzoic acid (Rohles et al., 2022). In selected experiments, the medium was additionally supplemented with aromatic compounds from filter-sterilized stocks: caffeic acid, CAF; *p*-coumaric acid, COU; 3,

Table 1
Strains and plasmids used in this study.

Strains/ Plasmids	Description	Reference
Strains		
E. coli		
DH10B	Vector amplification and maintenance	Korneli et al. (2013)
NM522 + pTC	Vector amplification and methylation	Kind et al. (2010)
C. glutamicum		
ATCC 13032	Wildtype	Becker et al. (2018a)
MA-2	Wildtype + deletion of *catB* (*NCgl2318*) + overexpression of *catA* (*NCgl2319*) under control of P_{tuf} (*NCgl0480*)	Becker et al. (2018a)
Δ*fudC*	Wildtype + deletion of *fudC* (*NCgl0324*)	This work
Δ*adhP*	Wildtype + deletion of *adhP* (*NCgl2709*)	This work
Δ*vanK*	Wildtype + deletion of *vanK* (*NCgl2302*)	This work
MA-3	MA-2 + deletion of *fudC* (*NCgl0324*)	This work
MA-4	MA-2 + overexpression of *vdh* (*NCgl2578*) under control of P_{tuf}	This work
MA-5	MA-3 + overexpression of *vdh* (*NCgl2578*) under control of P_{tuf}	This work
MA-6A	MA-2 + integration of native *aroY* (*Ecl_01944*), *ecdB* (*Ecl_04083*), and *ecdD* (*Ecl_04081*) from *E. cloacae* under control of P_{tuf} into the *pcaG* locus (*NCgl2314*)	This work
MA-6B	MA-2 + integration of codon-optimized *aroY* (*Ecl_01944*), *ecdB* (*Ecl_04083*), and *ecdD* (*Ecl_04081*) from *E. cloacae* under control of P_{tuf} into the *pcaG* locus	This work
MA-6C	MA-2 + integration of native *aroY* (*Kpn_01161*), *kpdB* (*Kpn_03098*), and *kpdD* (*Kpn_03096*) from *K. pneumoniae* under control of P_{tuf} into the *pcaG* locus	This work
MA-6D	MA-2 + integration of codon-optimized *aroY* (*Kpn_01161*), *kpdB* (*Kpn_03098*), and *kpdD* (*Kpn_03096*) from *K. pneumoniae* (ATCC 700721) under control of P_{tuf} into the *pcaG* locus	This work
MA-6E	MA-2 + integration of native *aroY* (*NYB75845.1*), *shdB* (*AAY67850*), and *shdD* (*AAY67851*) from *S. hydroxybenzoicus* under control of P_{tuf} into the *pcaG* locus	This work
MA-6F	MA-2 + integration of codon-optimized *aroY* (*NYB75845.1*), *shdB* (*AAY67850*), and *shdD* (*AAY67851*) from *S. hydroxybenzoicus* under control of P_{tuf} into the *pcaG* locus	This work
MA-7	MA-5 + integration of native *aroY* (*Ecl_01944*), *ecdB* (*Ecl_04083*), and *ecdD* (*Ecl_04081*) from *E. cloacae* under control of P_{tuf} into *pcaG*	This work
MA-8	MA-5 + deregulation of *vanABK (NCgl2300-NCgl2302)* by deletion of *vanR* (*NCgl2299)* and overexpression of *vanABK* under control of P_{tuf}	This work
MA-9	MA-8 + integration of native *aroY* (*Ecl_01944*), *ecdB* (*Ecl_04083*), *ecdD* (*Ecl_04081*) from *E. cloacae* under control of P_{tuf} into the *pcaG* locus	This work
Plasmids		
pTC	Vector for DNA-methyltransferase of *C. glutamicum* with an origin of replication for *E. coli* and tet^R as selection marker	Kind et al. (2010)
pClik int SacB	Integrative vector with a MCS, an ORI for *E. coli*, and kan^R and *sacB* as selection markers	Kind et al. (2010)
pClik int SacB Δ*fudC*	Deletion of *fudC*	This work
pClik int SacB P_{tuf} *vdh*	Replacement of the native promoter of *vdh* by P_{tuf}	This work
pClik int SacB P_{tuf} *vanABK: vanR*	Replacement of the native promoter of *vanABK* by P_{tuf} with simultaneous deletion of *vanR*	This work
pClik int SacB Δ*vanK*	Genomic deletion of *vanK*	This work
pClik int SacB P_{tuf} *aroY ecdBD*^{opt}	Genomic integration of codon-optimized *aroY* and *ecdBD* from *E. cloacae* under control of P_{tuf} into the *pcaG* locus	This work
pClik int SacB P_{tuf} *aroY ecdBD*^{nat}	Genomic integration of native *aroY and ecdBD* from *E. cloacae* under control of P_{tuf} into the *pcaG* locus	This work
pClik int SacB P_{tuf} *aroY kpdBD*^{opt}	Genomic integration of codon-optimized *aroY* and *kpdBD* from *K. pneumoniae* under control of P_{tuf} into the *pcaG* locus	This work
pClik int SacB P_{tuf} *aroY kpdBD*^{nat}	Genomic integration of native *aroY* and *kpdBD* from *K. pneumoniae* under control of P_{tuf} into the *pcaG* locus	This work
pClik int SacB P_{tuf} *aroY shdBD*^{opt}	Genomic integration of codon-optimized *aroY* and *shdBD* from *S. hydroxybenzoicus* under control of P_{tuf} into the *pcaG* locus	This work
pClik int SacB P_{tuf} *aroY shdBD*^{nat}	Genomic integration of native *aroY and shdBD* from *S. hydroxybenzoicus* under control of P_{tuf} into the *pcaG* locus	This work

4-dihydroxybenzaldehyde (protocatechualdehyde), PAL; 3,4-dihydroxybenzoic acid (protocatechuic acid), PCA; 3,4-dihydroxybenzyl alcohol (protocatechuyl alcohol), PLC; ferulic acid, FER; *p*-hydroxybenzaldehyde, HAL; *p*-hydroxybenzoic acid, HBA; *p*-hydroxybenzyl alcohol; HLC; vanillic acid, VNA; vanillin, VIN; vanillyl alcohol, VLC, as given below. In addition, softwood derived EuroVanillin (Batch no: 19FKG5010) was used, kindly provided by the commercial supplier (Borregaard, Sarpsborg, Norway).

2.4. Batch cultivation of *C. glutamicum* in shake flasks

For characterization purposes, the cultivation procedure comprised two successive pre-cultures, followed by one main-culture, all incubated in baffled shake flasks with 10% filling volume on an orbital shaker at 230 rpm and 30°C (Multitron, Infors-HT, Bottmingen, Switzerland; shaking diameter: 5 cm). For the first pre-culture, 10 mL BHI-complex-medium was inoculated from a single colony of a BHI-agar plate, which had been pre-incubated for 48 h at 30°C. From there, the second pre-culture and the main culture were conducted in 25 mL minimal medium, whereby the aromatic biotransformation substrate was only added to the main culture. Prior to inoculation of the second pre-culture and the main culture, cells were harvested by centrifugation (6,000×*g*, 4 min, RT). All experiments were done as biological triplicate.

2.5. Screening of *C. glutamicum* in a micro bioreactor

Alternatively, for screening purposes (e. g., tolerance assay), the main cultures were performed in a micro bioreactor (BioLector, Beckman Coulter GmbH, Baesweiler, Germany) in 48-well flower plates (MTP-48 B, Beckman Coulter GmbH). Using the same pre-culture medium as above, the main cultures were inoculated to an initial OD_{660} of 1 and grown for 24 h in 1 mL medium at 30°C, 1,300 rpm, and a relative humidity of 85% (Becker et al., 2018a). Cell growth was monitored on-line in the micro-bioreactor as optical density (OD_{620}), whereby the maximum specific growth rate for each tested condition was determined during the exponential growth phase by regression of $\ln(OD_{620})$ over time (Kohlstedt et al., 2022). Additionally, the tolerance was estimated based on the final OD_{660} that was measured photometrically as given below. For cases of biphasic growth profiles, the specific growth rate was inferred during the major growth phase, attributed to glucose-associated biomass formation. All cultivation conditions were tested in biological triplicates.

2.6. Quantification of cell concentration, substrates, and products

The cell concentration was determined as optical density at 660 nm (OD_{660}). If necessary, internal blanks were generated by centrifugation from non-inoculated controls (13,300×*g*, 3 min, 4°C), and used as

reference to correct for absorbance effects by certain aromatics (e. g., caffeate, protocatechualdehyde). For the calculation of cell dry mass (CDM) from OD_{660} values, the following correlation was used: CDM [g L^{-1}] = 0.32 x OD_{660} (Rohles et al., 2016).

Glucose was quantified by isocratic HPLC (1260 Infinity Series, Agilent Technologies, Waldbronn, Germany) (Hoffmann et al., 2018). In short, separation was performed using a Metacarb 87C guard column (7.8 × 50 mm, Agilent), and an analytical Metacarb 87C column (7.8 × 300 mm, Agilent) at 85°C as the stationary phase and deionized water at a flow rate of 0.5 mL min^{-1} as the mobile phase. Glucose was detected by refraction index measurement at 55°C (Agilent 1260 RID G12362A, Agilent Technologies) and quantified using external standards.

Aromatics and MA were analyzed by HPLC (1260 Infinity Series, Agilent Technologies). For separation at 25°C, a pre-column (Nucleodur EC4/3 C18 Isis, 3 μm, 4 mm, Macherey-Nagel, Düren, Germany) and an analytical C18 column (Nucleodur EC 100/3 C18 Isis, 3 μm, 100 mm, Macherey-Nagel) were used, applying the following gradient of 0.025% phosphoric acid (eluent A) and acetonitrile (eluent B) at a constant flow rate of 1 mL min^{-1}: 0-13.8 min, 99–67% A; 13.8–14.3 min, 67–0% A; 14.3–17.3 min, 0% A; 17.3–17.8, 0–99% A; 17.8–24.3 min, 99% A. The analytes were detected by UV absorption at compound-specific wavelengths, corresponding to individual absorption maxima: 200 nm for vanillyl alcohol, *p*-hydroxybenzaldehyde, *p*-hydroxybenzyl alcohol, protocatechualdehyde, and protocatechuyl alcohol; 210 nm for protocatechuate, catechol, *p*-hydroxybenzoate; 220 nm for vanillate; 230 nm for vanillin; 260 nm for MA; 310 nm for *p*-coumarate, and 325 nm for caffeate and ferulate (Agilent 1260 DAD, G4212B, Agilent Technologies). For quantification, external standards were applied.

2.7. Structural identification of unknown pathway intermediates by GC-MS

Aromatic metabolites were identified by GC-MS analysis after conversion into *t*-butyl-trimethylsilyl-derivatives (Barton et al., 2018). In short, 20 μL supernatant was dried under a nitrogen stream, dissolved in 50 μL dimethylformamide (0.1% pyrimidine) and amended with 50 μL N-methyl-N-(*t*-butyl-dimethylsilyl)trifluoroacetamide (Macherey and Nagel) to yield the silylated derivatives. After incubation for 30 min at 80 °C, the obtained products were analyzed (GC/MS 7890A, 5975C quadrupole detector, Agilent Technologies) using an HP-5MS capillary column (30 m × 250 μm x 0.25 μm, (5%-phenyl)-methyl-polysiloxane, Agilent Technologies), and electron impact ionization at 70 eV (Wittmann et al., 2002). Helium 5.0 was used as carrier gas at a flow rate of 1.7 mL min^{-1}. For analysis, 1 μL sample was injected in split mode (split ratio, 30:1; split flow, 51 ml min^{-1}). The temperature gradient for separation of the analytes was 120°C for 2 min, 8°C min^{-1} up to 200°C, and 10°C min^{-1} up to 325°C for 2.5 min. Further process-relevant temperature settings were 250°C (inlet), 280°C (transfer line), 230°C (ion source), and 150°C (quadrupole). The mass spectra of the analytes were collected in scan mode over an *m/z* range of 50–750 and were compared to the National Institute of Standards and Technology (NIST) library (version: NIST08). As reference, pure standards were derivatized and analyzed as described above.

3. Results and discussion

3.1. C. glutamicum exhibits high tolerance to vanillin and vanillate, the major aromatics from alkaline-oxidized softwood lignin

Obviously, high robustness against aromatics is a key requirement to harness microorganisms in the context of lignin valorization (Becker and Wittmann, 2019), which also held true for vanillin and vanillate, the two predominant monomers that result from alkaline oxidation of softwood lignin (Bjørsvik and Minisci, 1999; Fache et al., 2016; Pacek et al., 2013; Rødsrud, 2018). *C. glutamicum* appeared as a promising choice, given its recently demonstrated capability to produce MA from benzoate, catechol and phenol (Becker et al., 2018a), and its generally broad aromatic substrate spectrum (Fig. 1A), including *inter alia* vanillin (Ding et al., 2015) and also vanillate (Merkens et al., 2005).

We first evaluated the capacity of the *C. glutamicum* wildtype to assimilate vanillin (Fig. 1B) and vanillate (Fig. 1D) in the presence of glucose, thereby mimicking the previously reported MA-production conditions (Becker et al., 2018a). Vanillin had only a minor inhibitory impact on *C. glutamicum* (Fig. 1B, Fig. S1, Supplementary File 1). The microbe could well grow up to the highest tested concentration of 30 mM vanillin and the biomass remained nearly unaffected up to 20 mM. The tolerance to high vanillin levels was to some extent surprising, given that this aromatic is known as particularly toxic (Pattrick et al., 2019) and one of the major inhibitors in pre-treated lignocellulose (Chen et al., 2016). Vanillate was found even less inhibitory than vanillin (Fig. 1D, Fig. S1, Supplementary File 1). Both aromatics were also efficiently consumed. Up to a level of 10 mM, about 50% of the vanillin was consumed within 24 h, while vanillate was even completely removed (Fig. 1C and E). This in-built tolerance of *C. glutamicum* against the two aromatics was remarkable and appeared advantageous for the start.

Interestingly, a more detailed analysis of the cultures unveiled an unknown substance that accumulated in the supernatant of all vanillin-based cultures over time. The compound was neither formed by vanillate-grown cells nor in uninoculated controls, pointing to a vanillin-associated biological origin. During HPLC analysis, the unknown metabolite (4.6 min) eluted before vanillate (6.4 min) and vanillin (7.5 min), suggesting a molecule with high polarity (Fig. S2A, Supplementary File 1).

3.2. Vanillin-grown C. glutamicum forms substantial levels of vanillyl alcohol as a dead-end product

The compound, produced by vanillin-grown cells, deserved further attention. GC-MS analysis of vanillin-based culture supernatant (Fig. S2B, Supplementary File 1) identified it as vanillyl alcohol, matching recent reports (Kim et al., 2022; Zhou et al., 2022). When subsequently quantified, it turned out about 50% of vanillin was converted into vanillyl alcohol instead of being catabolized (Fig. 1C). According to previous studies (Priefert et al., 2001), vanillyl alcohol formation is known to be a detoxification mechanism in vanillin-grown bacteria (Fleige et al., 2016; García-Hidalgo et al., 2020; Meyer et al., 2018; Zhou et al., 2022; P. Zhou et al., 2019a), yeasts (Hansen et al., 2009), and fungi (Shimizu et al., 2005). For vanillin-grown *C. glutamicum,* formation of the (apparently less toxic) alcohol turned out to be a part of a complex cell response which furthermore involved *inter alia* changes of the cell envelope, and an up-regulation of stress response genes, as shown before (Chen et al., 2016).

Taken together, *C. glutamicum* exhibited a branched vanillin metabolism, consisting of an oxidative route to vanillate and a reductive route to the corresponding alcohol. When studied over time, formation of vanillyl alcohol started immediately upon inoculation and was linked to the consumption of vanillin (Fig. 2A). When all vanillin had been consumed after 12 h, more than one half of the initially supplied substrate was detected as vanillyl alcohol (0.57 ± 0.01 mol mol^{-1}), and, interestingly, the by-product remained almost untouched during further incubation (0.54 ± 0.00 mol mol^{-1} after 24 h). Thus, it appeared that vanillin, once reduced into vanillyl alcohol, was no more efficiently accessible to *C. glutamicum*. This observation was substantiated by a cultivation of the wildtype strain on glucose and vanillyl alcohol, where only a minor fraction of the alcohol was consumed (Fig. 2B). Surprisingly, this behavior differed from that of other bacteria. A *Pseudomonas* isolate (Ravi et al., 2018) and *C. glutamicum* S9114 (P. Zhou et al., 2019a) were both reported to efficiently take up vanillyl alcohol in later stages of vanillin-based cultivations. All in all, substantial amounts of vanillyl alcohol were formed by vanillin-grown *C. glutamicum* in a typical MA-producing setup (Becker et al., 2018a). Thus, the natural defense of the microbe caused an unfavorable loss of the aromatic

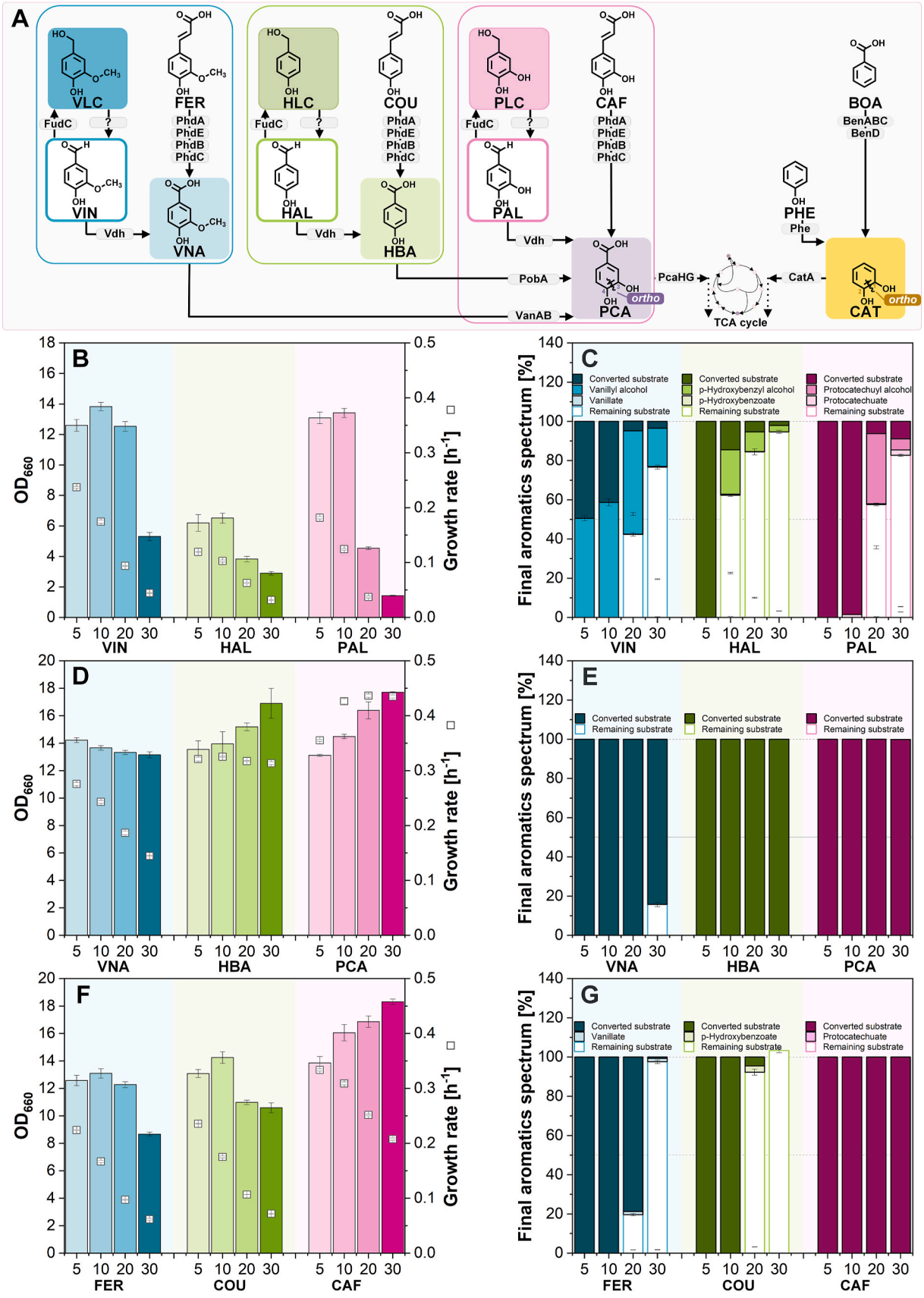

(caption on next page)

Fig. 1. Potential of *Corynebacterium glutamicum* for the valorization of structurally diverse lignin-derived aromatic compounds. A: native catabolic pathways of the microbe to degrade aromatic compounds taken from previous studies (Ding et al., 2015; Huang et al., 2008; Kallscheuer et al., 2016; Merkens et al., 2005; Shen et al., 2012; Xiao et al., 2015) and new findings in this work. The aromatics are representative for compounds obtained during lignin depolymerization (blue, G-lignin substitution; green, H-lignin substitution; pink, C-lignin substitution) (Vermaas et al., 2019). B: Metabolization of varied concentrations (5, 10, 20, 30 mM) of aromatic aldehydes (B, C), aromatic acids (D, E) and hydroxycinnamates (F, G) by the wildtype, with additionally 55 mM glucose. The cultures were conducted in a 48-well plate micro bioreactor with on-line monitoring of growth. The corresponding growth profiles can be found in the **Supplementary File 1**. The tolerance of the microbe against the aromatics was estimated from the final cell concentration after 24 h measured at 660 nm and the specific growth rate measured online during the major growth phase (B, D, F). In addition, concentration changes of substrates and products were analyzed by end point measurements. The decrease of caffeate and protocatechualdehyde was probably superimposed by abiotic oxidation (**Supplementary File 1**). The data represent mean values and standard deviations from three biological replicates. Abbreviations: CAF – caffeate, COU – *p*-coumarate, FER – ferulate, HAL – *p*-hydroxybenzaldehyde, HBA – *p*-hydroxybenzoate, HLC – *p*-hydroxybenzyl alcohol, PAL – protocatechualdehyde, PCA – protocatechuate, PLC – protocatechuyl alcohol, VIN – vanillin, VLC – vanillyl alcohol, VNA – vanillate.

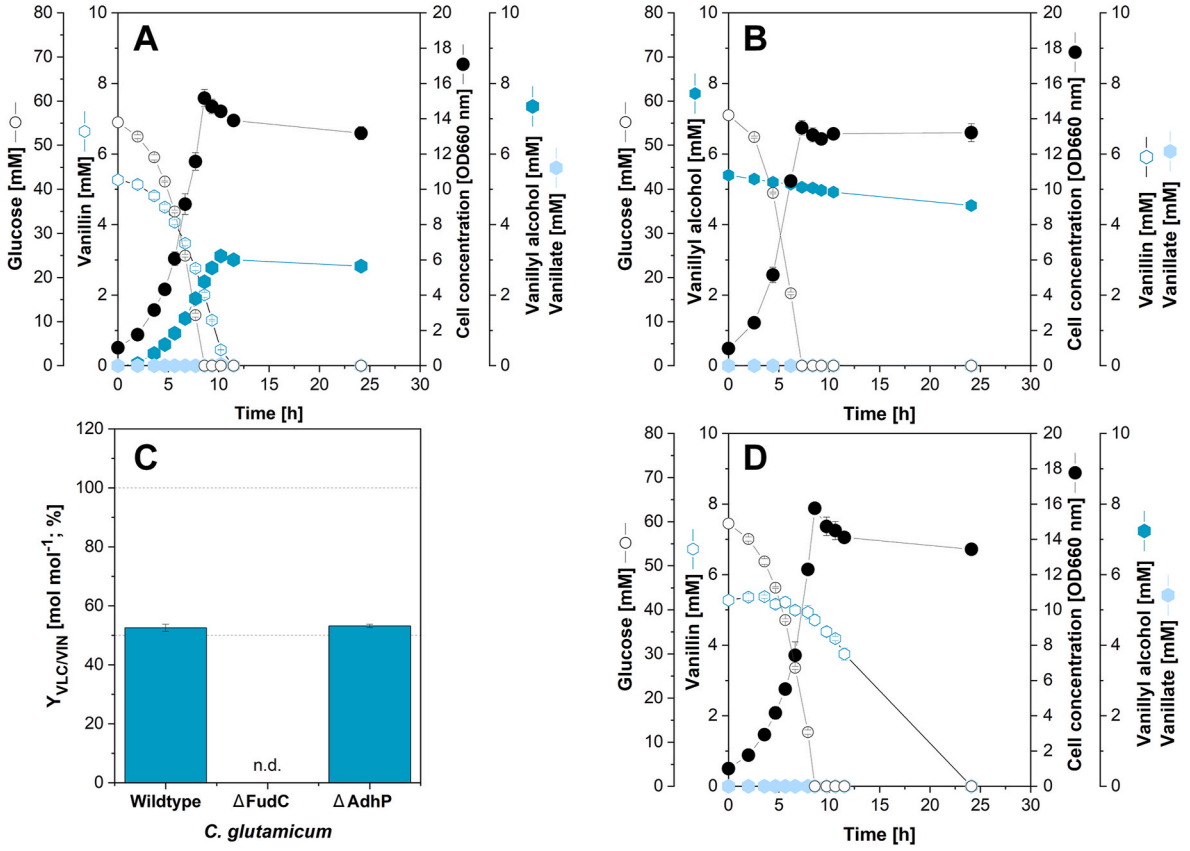

Fig. 2. Characterization of the branched vanillin metabolism in *C. glutamicum*. Culture profiles of the wildtype strain on 5 mM vanillin (A) and 5 mM vanillyl alcohol (B), each supplemented by 55 mM glucose. To identify the enzyme responsible for vanillin reduction, BLASTP-analysis was performed using AreA (PP_2426) from *P. putida* KT2440 (García-Hidalgo et al., 2020) as a template. Subsequently, the wildtype and two deletion mutants, namely *ΔfudC* and *ΔadhP* were cultivated for 24 h on 5 mM vanillin and 55 mM glucose in a micro bioreactor (C). Strain *C. glutamicum ΔfudC* did not produce vanillyl alcohol (VLC) from vanillin (VIN) (C). The culture profile of *C. glutamicum ΔfudC* on 5 mM vanillin, supplemented by 55 mM glucose (D), additionally, suggested that FudC is the only active vanillin reductase in *C. glutamicum* for the tested experimental setup. The data comprise mean values and deviations from three biological replicates.

substrate into a dead-end product, displaying a major drawback towards valorizing vanillin into MA.

3.3. Discovery and deletion of FudC eliminates vanillyl alcohol formation but unveils a natural deficiency of C. glutamicum to oxidize and catabolize vanillin

The formation of vanillyl alcohol from vanillin made the identification (and elimination) of the unknown vanillin-reducing enzyme(s) an important next step. To this end, we conducted a BLASTP analysis against the protein repertoire of *C. glutamicum* (Altschul, 1997; Altschul et al., 2005) using the amino acid sequence of another aromatic aldehyde reductase as a template, namely that of the recently identified enzyme AreA (PP_2426) from *P. putida* KT2440 (García-Hidalgo et al., 2020). The search suggested several candidates (Table S3, Supplementary File 1). Two of them appeared most promising: (i) the Zn-dependent alcohol dehydrogenase FudC (NCgl0324), previously shown to reduce furfural into furfuryl alcohol (Tsuge et al., 2016) and to be of relevance for aromatic aldehyde production (Kim et al., 2022), which exhibited the highest identity (49%) and the best E-value, and (ii), the alcohol dehydrogenase AdhP (NCgl2709), showing still reasonable 30% identity, which was reported to be transcriptionally induced in vanillin-grown *C. glutamicum* (Chen et al., 2016). To study their contribution to vanillin reduction, both genes were individually deleted in the wildtype. The newly constructed mutants *C. glutamicum ΔfudC* and *ΔadhP* lacked the entire sequence of *fudC* and *adhP*, respectively, as verified by PCR and sequencing. They were both cultivated on glucose and vanillin, along with the wildtype as control (Fig. 2C). Favorably, vanillyl alcohol was no more formed in the *ΔfudC* mutant, demonstrating that FudC was the only active vanillin reductase in

C. glutamicum, different to *R. opacus* PD630, where more than one enzyme contributes to vanillyl alcohol formation (Zhou et al., 2022). *C. glutamicum ΔadhP* revealed an unchanged vanillin metabolism, well matching this picture (Fig. 2C).

Subsequently, we studied the consequence of the *fudC*-deletion in more detail over time (Fig. 2D). Vanillyl alcohol formation was not apparent in any cultivation stage, further confirming that FudC exclusively catalyzed vanillin reduction in *C. glutamicum*. However, *C. glutamicum* Δ*fudC* exhibited an impaired consumption of vanillin. Unfavorably, the (undoubtedly important) mutation introduced a new bottleneck. In conclusion, natural vanillin degradation in *C. glutamicum* largely relied on rapid reduction into the alcohol, i.e., *via* the reductive vanillin branch. The oxidative branch alone, where vanillin was oxidized into vanillate (Figs. 1 and 2D), did not offer sufficient catabolic capacity to ensure efficient assimilation, leaving space for improvement. Interestingly, *R. opacus* PD630, another *Actinobacterium*, exhibits a similar natural deficiency to oxidize vanillin, and was reported to produce vanillyl alcohol as a dead-end metabolite (Zhou et al., 2022), eventually indicating shared metabolic traits between different *Actinobacteria* regarding their vanillin metabolism.

3.4. Metabolic engineering of a high flux module for improved vanillin assimilation

Next, we aimed to increase the vanillin flux to protocatechuate, a central precursor for vanillin-based MA-production (Fig. 2). From here on (Fig. 3, Fig. S3, Supplementary File 1), metabolic engineering focused on upgrading the basic MA-producer *C. glutamicum* MA-2 (Becker et al., 2018a). One should note that MA-2 and derivatives, created therefrom at this stage, were not yet able to directly produce MA from vanillin but catabolized the aromatic for growth instead. This layout offered to streamline vanillin catabolism without being potentially impacted by an artificially introduced downstream bottleneck. To improve the use of vanillin, we explored different strategies that aimed at an outbalancing of its branched metabolism (Fig. 4, Fig. S4, Supplementary File 1).

First, we deleted *fudC* in MA-2 using the same integrative plasmid as before. Two rounds of recombination, validated by PCR and sequencing for a correct genomic elimination of *fudC*, yielded the derivative strain MA-3. Even though vanillyl alcohol formation was diminished, the deletion of *fudC*, also unfavorably, affected strain tolerance when approaching higher vanillin levels, which was reflected in lower growth rates compared to MA-2 (Fig. 4B). Additionally, MA-3 exhibited a limited capacity to oxidize vanillin, matching the overall picture for *C. glutamicum* Δ*fudC* (Fig. 2D).

Second, we focused on the optimization of the obviously limited conversion of vanillin into vanillate (Fig. 4B). Based on sequence-based identification as vanillin dehydrogenase (Shen et al., 2012) and detailed functional characterization (Ding et al., 2015), we overexpressed the gene *vdh* (*NCgl25789*) in strain MA-2. For this purpose, the natural *vdh* promotor was replaced by the strong, constitutive *tuf* promoter (P_{tuf}), which is well known to enable an upregulation of different genes of interest in *C. glutamicum* (Becker et al., 2005, 2011). The cloning, followed by PCR and sequencing validation, yielded *C. glutamicum* MA-4. Favorably, overexpression of *vdh* increased the growth rate on vanillin and even reduced vanillyl alcohol formation at lower vanillin level (Fig. 4B). However, the sole promotion of the oxidative pathway was not sufficient to fully avoid the undesired alcohol accumulation.

Therefore, we combined the deletion of *fudC* with the overexpression of *vdh*, which was realized by replacing the natural *vdh* promotor by the *tuf* promotor in MA-3. The newly constructed mutant MA-5 carried both desired changes, as verified by PCR and sequencing. Nicely, MA-5 did not produce vanillyl alcohol, even at the highest vanillin concentration (Fig. 4B). The novel mutant also grew significantly better than its parent derivative MA-3 (Fig. 4B). When approaching higher vanillin concentrations (20 mM), we even observed an accumulation of vanillate, which revealed the desired shift from the naturally dominant reductive to the oxidative pathway.

3.5. High-efficiency coupling of aromatic degradation and product biosynthesis: Discovery of the optimal protocatechuate module

The excretion of excess vanillate in vanillin-grown *C. glutamicum* MA-5 was a valuable indication that sufficient precursor was available to be re-directed by further engineering rounds towards MA. For both *de novo* synthesis of MA from glucose (Draths and Frost, 1994) and biotransformation of aromatic compounds, degraded *via* protocatechuate, into MA (Sonoki et al., 2014; Vardon et al., 2015), the protocatechuate decarboxylase AroY, which decarboxylates protocatechuate into the MA-precursor catechol, acts as a key enzyme (Fig. 3). Likewise, *C. glutamicum* degraded vanillin and vanillate *via* protocatechuate, which required to efficiently re-direct the aromatics to the catechol node (Figs. 1 and 3). It goes without saying that this metabolic step is crucial, which explains why practically every study, aiming at this conversion, had to search for an individual layout that best addressed the used microbe as well as substrates and process conditions. Most studies so-far relied on the AroY variants from Gram-negative *Enterobacter cloacae* (Leavitt et al., 2017; Vardon et al., 2015) and *Klebsiella pneumoniae* (Draths and Frost, 1994; Sonoki et al., 2018; Weber et al., 2012), and the latter variant also found application in *C. glutamicum* for *de novo* MA synthesis from glucose, where it was tested as the only candidate (Lee et al., 2018). Here we included both enzymes for the envisioned pathway coupling. Additionally, we tested an AroY variant from a Gram-positive donor, taxonomically more related to *C. glutamicum*. The Gram-positive bacterium *Sedimentibacter hydroxybenzoicus* was known to contain an (admittedly oxygen-sensitive) protocatechuate decarboxylase, named ShdC (Weber et al., 2012). The strain obviously further possessed an AroY homologue (He and Wiegel, 1996), similar to other bacteria possessing protocatechuate decarboxylases (Sonoki et al., 2014; Weber et al., 2012), not yet tested for MA production. We identified the corresponding *aroY* gene in the genome of *S. hydroxybenzoicus via* BLASTP analysis (Tables S4 and S5, Supplementary File 1). The protein revealed a good conversation of amino acid residues, putatively involved in the AroY catalytic mechanism (Payer et al., 2017) (Fig. S5, Supplementary File 1).

The *aroY*-variants from *K. pneumoniae*, *E. cloacae*, and *S. hydroxybenzoicus,* respectively, were individually introduced, together with two accessory *B* and *D* genes (Erickson et al., 2022), from the respective *aroY*-donors (Table 1). In each case, the three genes were genomically introduced into *C. glutamicum* MA-2 (Becker et al., 2018a) as a single monocistronic module under control of P_{tuf}. To simultaneously prevent natural protocatechuate catabolization, *pcaG*, encoding the protocatechuate 3,4-dioxygease α-subunit, was selected as the integration locus (Shen and Liu, 2005). Within the modules, the three genes were separated by ribosomal binding sites (Rohles et al., 2016, 2018) (Fig. 3, Fig. S3, Supplementary File 1). For each *aroY*-variant, native and codon-optimized gene versions were synthesized and tested. The sequences of all genes (optimized and native) are given in the supplement (Table S2, Supplementary File 1). The (altogether six) mutants, designated MA-6A to MA-6F, were obtained in two rounds of recombination (Table 1). Prior to further investigation, they were all validated thoroughly for correctness of the introduced genetic modification using PCR and sequencing.

Each strain was then cultivated in a biotransformation setup with different protocatechuate levels plus glucose. The established protocatechuate decarboxylase activity was assessed on basis of MA, produced after 24 h (Fig. 5). Out of all designs, *C. glutamicum* MA-6A and MA-6B, expressing the *E. cloacae*-variant, performed best. Even the highest protocatechuate concentration (30 mM) was almost completely converted into MA. Hereby, the native gene version seemed slightly more efficient (Fig. S6, Supplementary File 1). In comparison, the *aroY* gene from *K. pneumoniae* worked less efficient. The corresponding strains MA-6C and MA-6D converted protocatechuate only partially and

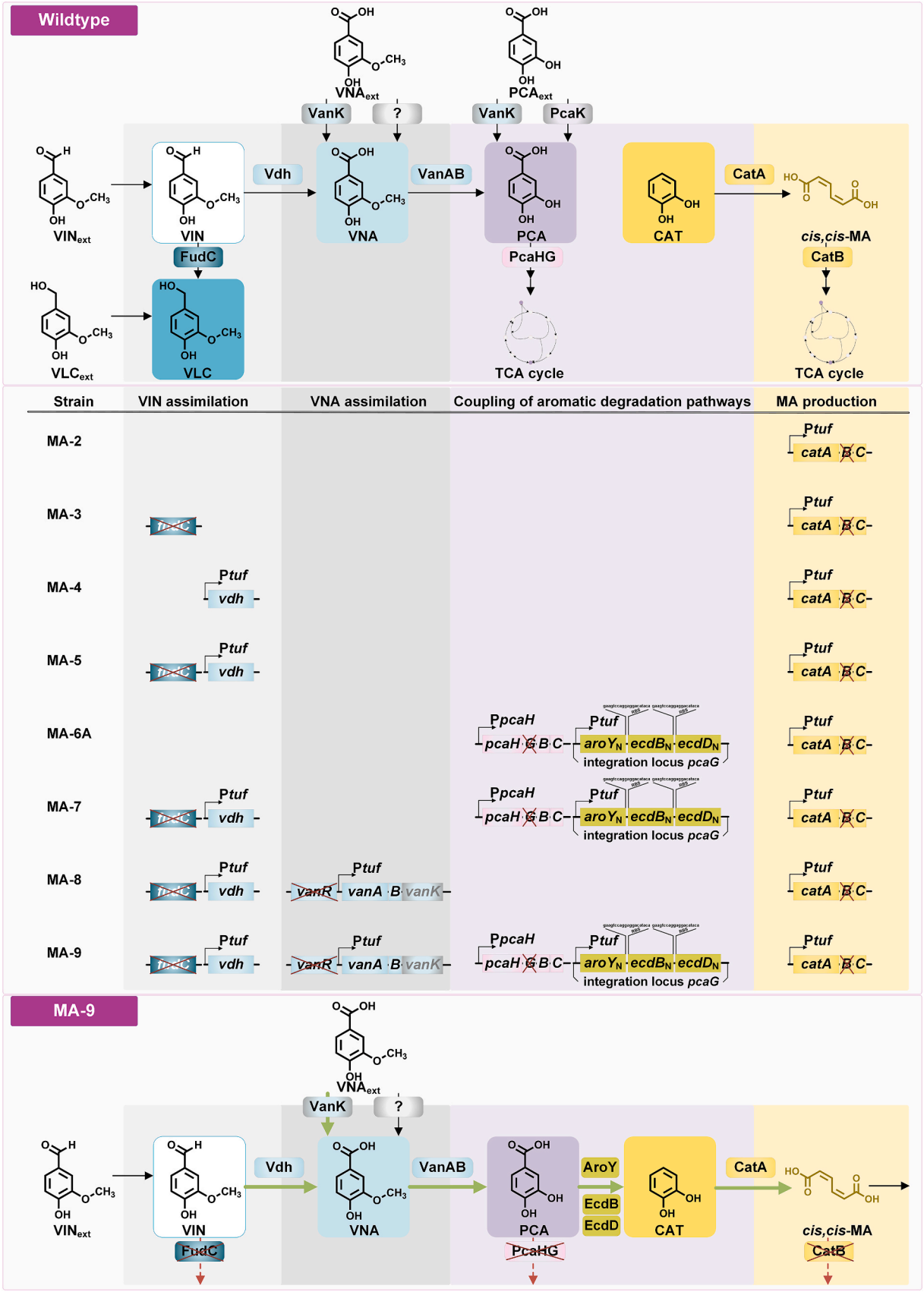

(caption on next page)

Fig. 3. Metabolic pathway design for vanillin- and vanillate-based MA-production in *C. glutamicum*. The overview illustrates the native metabolism of selected aromatic compounds in the wildtype (A) and the genomic layout of engineered strains from several rounds of systems metabolic engineering towards enhanced vanillin and vanillate assimilation, followed by the coupling of both branches of the β-ketoadipate pathway towards MA production (B). All modifications were implemented into the genome, whereby strain MA-2 from our previous work served as a starting point for further metabolic engineering (Becker et al., 2018a). The final producer *C. glutamicum* MA-9 (C) is featured by (i) the deletion of *fudC*, encoding a promiscuous aromatic aldehyde reductase to prevent vanillyl alcohol formation, (ii) the overexpression of *vdh*, encoding vanillin dehydrogenase, to promote oxidative vanillin metabolism, and (iii) *vanAB*, encoding vanillate-*O*-demethylase to abolish vanillate accumulation in vanillin-grown cells. Additionally, strain MA-9 expresses the native (N) variants of protocatechuate decarboxylase-encoding *aroY*, and the accessory genes *ecdBD* from *E. cloacae*, identified to be superior among homologous genes derived from *K. pneumoniae* and *S. hydroxybenzoicus*, all tested in native and codon optimized sequence versions. To prevent loss of protocatechuate towards central carbon metabolism, the genes were integrated into the *pcaG* locus, encoding for protocatechuate 3,4-dioxygenase alpha subunit. Based on this and recent studies, vanillate import probably takes place by VanK (Chaudhry et al., 2007), whereas protocatechuate import is likely mediated both by VanK as shown here and suggested before (Merkens et al., 2005), and PcaK (Chaudhry et al., 2007). An extended version of the tested genomic layouts, and the gene annotations, can be found in the supplementary material (Fig. S3, Supplementary File1). Deletion: red, dashed arrows. Overexpression: green, thick arrows. Abbreviations: CAT – catechol, MA – *cis, cis*-muconate, PCA – protocatechuate, VIN – vanillin, VLC – vanillyl alcohol, VNA – vanillate.

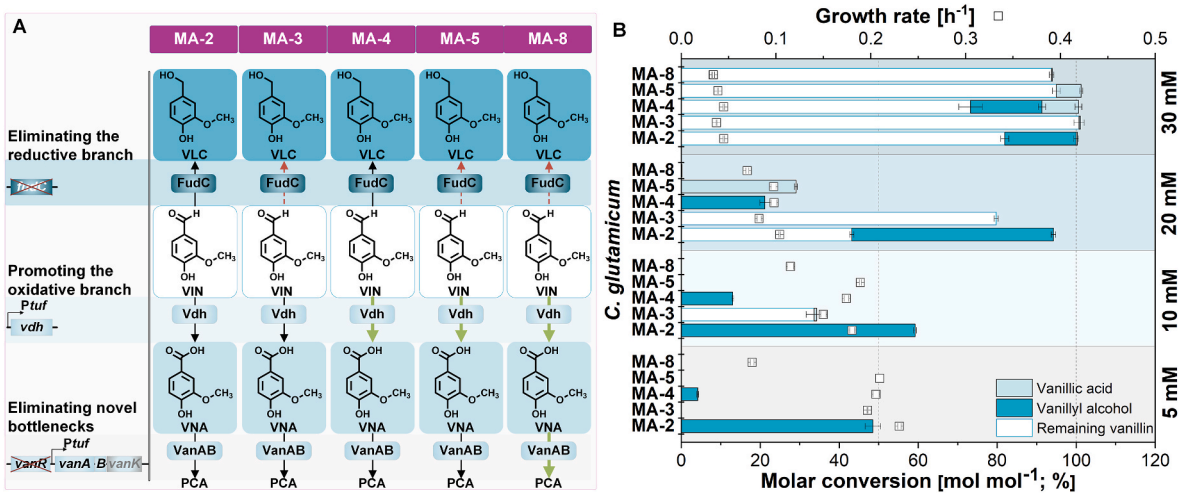

Fig. 4. Metabolic engineering of vanillin metabolism in *C. glutamicum* MA-2. After identifying a branched vanillin metabolism in *C. glutamicum*, different genomic layouts to achieve an optimal funneling of vanillin towards the oxidative branch were tested. The strategies involved (i) the elimination of the reductive branch by deleting *fudC* encoding for the newly discovered vanillin reductase (MA-3), (ii) the overexpression of vanillin dehydrogenase by the strong, constitutive *tuf*-promoter (MA-4), (iii) and a combinatory approach (MA-5). To counteract a synthetically introduced imbalance in vanillate assimilation, we, additionally, deregulated the *vanABK*-operon by introducing the strong, constitutive *tuf*-promoter with a simultaneous deletion of *vanR* (MA-8). Deletion: red, dashed arrows. Overexpression: green, thick arrows. (A). The different vanillin degraders MA-3, MA-4, MA-5 and MA-8 were cultivated on 55 mM glucose and varying vanillin concentrations (5, 10, 20, 30 mM) in a micro bioreactor. The effects of the different metabolic engineering strategies were evaluated based on end point measurements after 24 h. The data comprise mean values and deviations from three biological replicates. (B) Abbreviations: VIN – vanillin, VLC – vanillyl alcohol, VNA – vanillate.

accumulated less MA. Finally, the *aroY* gene from *S. hydroxybenzoicus* could be functionally expressed too, although only the native gene variant seemed to provide measurable activity. This protocatechuate decarboxylase (Fig. S5, Supplementary File 1) works best at high temperature (50°C) (He and Wiegel, 1996), a factor, which might have contributed to the low performance in *C. glutamicum*.

Taken together, the native *aroY* gene from *E. cloacae*, expressed together with the helper genes, emerged as the optimum protocatechuate module to channel flux from protocatechuate to MA. It strongly outcompeted the protocatechuate decarboxylase and its helper genes from *K. pneumoniae*, previously used in *C. glutamicum* to drive MA production from glucose (Lee et al., 2018) and was therefore selected for further strain engineering.

3.6. Combining the optimum vanillin and protocatechuate modules for vanillin-based MA-production

Next, we coupled the engineered vanillin and protocatechuate modules. Thus, the best-performing protocatechuate module, i.e., *aroY ecdBD*^{nat} from *E. cloacae*, was introduced into the improved vanillin degrader MA-5, resulting in strain MA-7. The mutant MA-7 and its parent strain MA-6A (with an unmodified vanillin metabolism for comparison) were cultivated on vanillin and glucose (Fig. 6). *C. glutamicum* MA-6A (Fig. 6A) strongly formed vanillyl alcohol and only weakly channeled the aromatic substrate towards MA. The aromatic alcohol was even the major product (Table 2), underlining to which extent the native detoxification competed with formation of the desired product.

C. glutamicum MA-7 performed tremendously better (Fig. 6B). It no longer accumulated vanillyl alcohol and revealed a stunningly improved vanillin metabolism, reflected by a more than 2-fold higher rate for vanillin uptake (Table 2). The MA production rate was even increased 7-fold. Although also the MA yield was substantially increased in strain MA-7 (by almost 40%), vanillin was still not entirely converted into the desired product, as would have been theoretically possible from the given pathway stoichiometry (Kohlstedt et al., 2018). The reason was a substantial accumulation of vanillate throughout the early production phase, and vanillate was still detected in elevated fractions in the supernatant, when vanillin had been entirely consumed (Table 2). This pointed out a newly emerging bottleneck at the level of vanillate-*O*-demethylase activity, similar to observations in other studies (Salvachúa et al., 2018; Sonoki et al., 2014; Vardon et al., 2015; Wu et al., 2018), thus, unveiling a new target for further strain improvement.

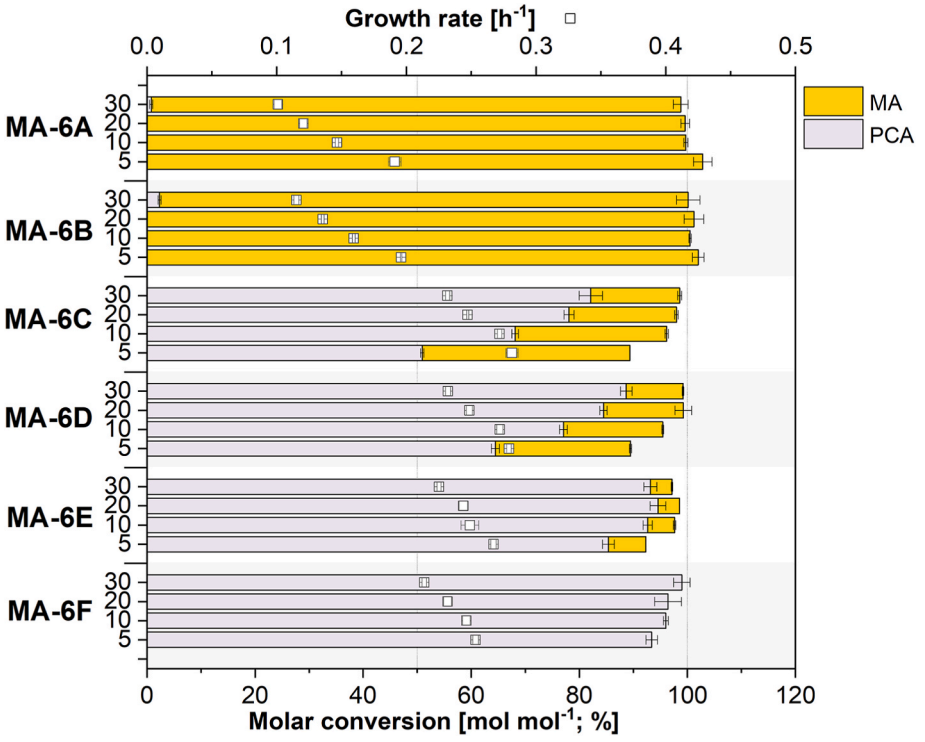

Fig. 5. Discovery of the optimum variant of protocatechuate decarboxylase AroY and associated helpers BD for production of MA from protocatechuate in *C. glutamicum* MA-2 through coupled catabolic and biosynthetic pathways. Codon-optimized (grey background) and native (white background) versions of *aroY* and its associated B- and D-genes from *E. cloacae*, *K. pneumoniae* and *S. hydroxybenzoicus*, were integrated under control of the *tuf*-promoter into the *pcaG*-locus of the MA-producer *C. glutamicum* MA-2. The strains were cultivated on 55 mM glucose and varying protocatechuate concentrations (5, 10, 20, 30 mM) in a microbioreactor. The different AroY-BD variants were compared based on end point measurements after 24 h, considering the produced muconate (MA) and the remaining, unconverted protocatechuate (PCA). The data comprise mean values and deviations from three biological replicates. The decrease of protocatechuate was probably also superimposed by abiotic oxidation (**Supplementary File 1**).

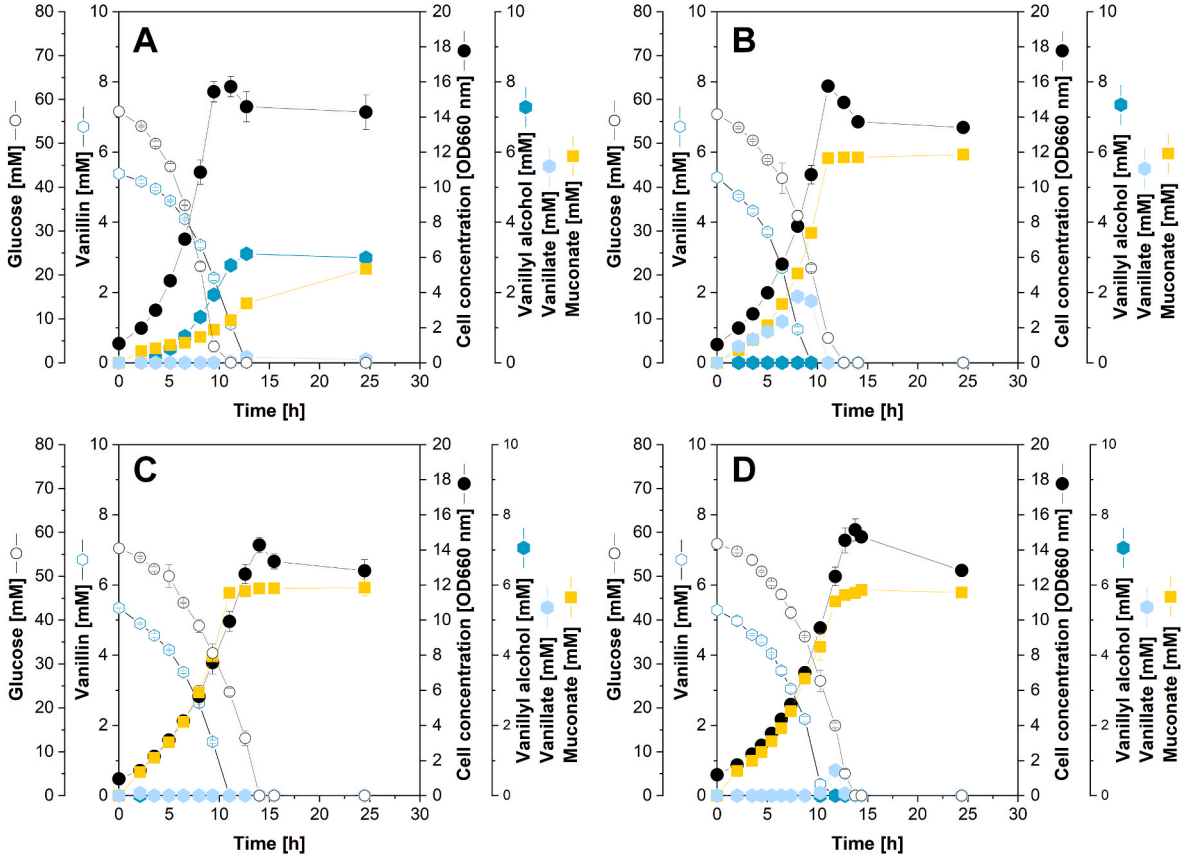

Fig. 6. Vanillin-based MA-production using metabolically engineered *C. glutamicum*. Cultivation profiles of the basic producer MA-6A (A), as well as the advanced producers MA-7 (B) and MA-9 (C) in co-presence of 5 mM vanillin and 55 mM glucose for growth. As a proof-of-concept, the best producer MA-9 with streamlined vanillin metabolism was, additionally, cultivated supplying 5 mM softwood-based EuroVanillin as biotransformation substrate (D). The data comprise mean values and deviations from three biological replicates.

Table 2
Growth and production performance of *C. glutamicum* strains engineered for vanillin- and vanillate-based MA production. The strains were cultivated in shake-flasks providing 55 mM glucose as growth substrate and 5 mM vanillin, wood-based vanillin (*), and vanillate as biotransformation substrate. Given are the specific rates for growth (μ), glucose uptake (q_{Glc}), vanillin/vanillate uptake (q_{ARO}), and MA production (q_{MA}), as well as the yields for biomass ($Y_{X/Glc}$), MA ($Y_{MA/VIN}$) and vanillin-associated metabolic by-products, including vanillyl alcohol ($Y_{VLC/VIN}$) and vanillate ($Y_{VNA/VIN}$). The yields $Y_{MA/ARO}$, $Y_{VLC/VIN}$ and $Y_{VNA/VIN}$ were determined for the sampling point where the entire amount of supplied aromatic biotransformation substrate was consumed, under consideration of the small amount of PCA available in the medium as complex agent. The given data represent mean values and standard deviations from three biological replicates.

Strain	WT_{VIN}	MA-$6A_{VIN}$	MA-7_{VIN}	MA-9_{VIN}	MA-9_{VIN}*	MA-$6A_{VNA}$	MA-9_{VNA}
Rates							
μ [h^{-1}]	0.32 ± 0.01	0.29 ± 0.01	0.23 ± 0.01	0.20 ± 0.00	0.20 ± 0.01	0.25 ± 0.00	0.12 ± 0.02
q_{Glc} [mmol g^{-1} h^{-1}]	3.97 ± 0.07	3.31 ± 0.13	2.55 ± 0.07	2.27 ± 0.07	2.30 ± 0.07	3.01 ± 0.14	1.91 ± 0.12
q_{ARO} [mmol g^{-1} h^{-1}]	0.23 ± 0.00	0.18 ± 0.01	0.42 ± 0.03	0.36 ± 0.03	0.37 ± 0.01	0.15 ± 0.00	0.43 ± 0.06
q_{MA} [mmol g^{-1} h^{-1}]	0.00 ± 0.00	0.04 ± 0.00	0.28 ± 0.02	0.37 ± 0.03	0.35 ± 0.02	0.17 ± 0.00	0.47 ± 0.00
Yields							
$Y_{X/Glc}$ [g $mmol^{-1}$]	0.08 ± 0.00	0.09 ± 0.00	0.09 ± 0.00	0.09 ± 0.00	0.09 ± 0.00	0.08 ± 0.00	0.06 ± 0.01
$Y_{MA/ARO}$ [mmol $mmol^{-1}$]		0.46 ± 0.01	0.64 ± 0.02	1.06 ± 0.01	1.02 ± 0.04	0.98 ± 0.02	1.05 ± 0.01
$Y_{VAL/VIN}$ [mmol $mmol^{-1}$]	0.51 ± 0.02	0.56 ± 0.02					
$Y_{VAT/VIN}$ [mmol $mmol^{-1}$]		0.02 ± 0.00	0.33 ± 0.02				

3.7. Finetuning of flux by a deregulated vanillate oxidation module allows stoichiometric conversion of vanillin into MA even at high concentration

To avoid vanillate accumulation (Fig. 6B), we designed a synthetic control of the two-component vanillate-*O*-demethylase VanAB, which catalyzed the oxidation of vanillate into protocatechuate (Merkens et al., 2005). In *C. glutamicum*, the catabolic genes *vanAB* form an operon together with *vanK* (Fig. 3), a putative protocatechuate (Merkens et al., 2005) or vanillate transporter (Chaudhry et al., 2007). Naturally, transcription of *vanABK* is locally regulated by the PadR-type repressor VanR (Morabbi Heravi et al., 2015). Thus, to enable synthetic control, we simultaneously deleted *vanR* and overexpressed the genes *vanABK* under P_{tuf} (Fig. 3).

This modification was first established in a non-MA-production background. When cultivated on glucose and varied vanillin levels, the new strain MA-8 did no longer accumulate vanillate, confirming that the chosen strategy worked well (Fig. 4B). Interestingly, MA-8 exhibited a rather unusual growth profile in comparison to its precursor strains with two sequential exponential growth phases (Fig. S4, **Supplementary File**).

Next, we equipped our so-far best producer MA-7 with the deregulated vanillate oxidation module, yielding strain MA-9, again validated by PCR and sequencing. Nicely, MA-9 produced MA free from vanillin without side-product (Fig. 6C), and, importantly, achieved the theoretical maximum MA yield of 100%, when vanillin was entirely consumed (Table 2). The synthetic control of the *van*-operon even further improved the product formation rate in comparison to the previous producer strain MA-7 by another 30%. Interestingly, the superiority in production characteristics came along with slightly slower growth and a slightly decreased uptake rate for both vanillin and glucose. These were probably secondary effects caused by the simultaneous overexpression of the transporter *vanK*, along with the *vanAB* genes, in line with previous reports that high-level expression of membrane proteins can impair the vitality of *C. glutamicum* (Rohles et al., 2022). Eventually, such an effect also caused the bi-phasic growth profile, shown above for MA-8.

3.8. Towards valorization of alkaline-oxidized softwood lignin, *C. glutamicum* MA-9 efficiently produces MA from vanillate and industrially lignin-derived vanillin

Next, strain MA-9 was benchmarked for MA-production from vanillate, the second major aromatic compound associated to alkaline depolymerization of softwood lignosulfonates (Fache et al., 2016; Pacek et al., 2013). We evaluated the advanced producer MA-9 on vanillate and glucose, whereby MA-6A served as reference (Fig. 7). The production performance of MA-9 was clearly superior. While both producers formed MA at stoichiometric yield, strain MA-9 accumulated the product 3-fold faster (Table 2). Interestingly, the novel mutant revealed a change in substrate preference. The uptake rate for vanillate was enhanced almost 3-fold, while the glucose assimilation rate was significantly decreased (Table 2), so that overall less glucose was required for MA-production, reflected in a higher $Y_{MA/GLC}$ (Fig. S7, Supplementary File 1). The enhanced vanillate uptake obviously resulted from the deregulated vanillate module, involving, *inter alia*, overexpression of *vanK*, previously reported to encode a vanillate importer (Chaudhry et al., 2007). It seemed that, further down the pathway, the activation of *vanABK* additionally triggered an, albeit small, protocatechuate accumulation (Fig. 7B).

On a first glance, the data seemed to provide a relatively clear mechanism for vanillate uptake in *C. glutamicum,* but other findings pointed to a more complex picture. Notably, a *vanK*-deletion mutant, constructed in this study (Table S1, Supplementary File 1), showed reduced protocatechuate uptake in comparison to the wildtype, whereas its vanillate uptake, surprisingly, was not affected, when grown on the respective aromatic carbon source as sole carbon and energy source (Fig. S8, Supplementary File 1). In line, VanK was supposed to be involved in protocatechuate transport in an earlier study (Merkens et al., 2005). Promiscuous transporters with shared substrate spectra, also comprising vanillate and protocatechuate, have been reported for other bacteria (D'Argenio et al., 1999; Mori et al., 2018; Wada et al., 2021). Future studies, including the search for eventually further involved transport proteins, could help to further resolve the picture in *C. glutamicum*, which could then enable elaborated transporter engineering towards enhanced MA-production from different aromatics, as in other current examples (Gómez-Álvarez et al., 2022; Mori et al., 2018; Wu et al., 2018).

To demonstrate end-to-end MA production from lignin, obtained through the alkaline depolymerization route, we cultivated our best producer *C. glutamicum* MA-9 on industrially derived lignin-based vanillin from softwood (Fig. 6D). The general growth and production performance of MA-9 on conventional vanillin and lignin-based vanillin was comparable (Table 2). Thus, vanillin was completely converted into MA after entire consumption of the biotransformation substrate. A slight vanillate accumulation was visible after 12 h, but the intermediate was fully taken up again at the next sampling point. Without doubt, this successful demonstration was an important proof-of-concept.

In the future, it would be interesting to test intermediate, less refined, streams from softwood biorefineries that operate alkaline oxidative depolymerization of softwood lignin at industrial scale (Rødsrud, 2018). Process streams, containing crude mixtures of vanillin and vanillate, as well as eventually other compounds (Fache et al., 2016; Pacek et al., 2013; Wouter Schutyser et al., 2018a) were not available in this study. Their evaluation would display an important next step towards a

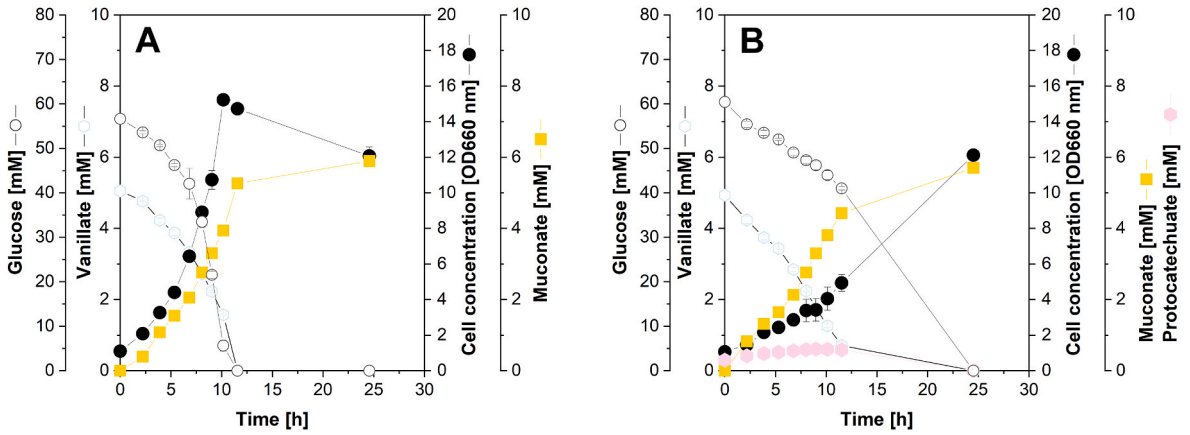

Fig. 7. Vanillate-based MA-production using metabolically engineered *C. glutamicum*. Cultivation profiles of the basic producer MA-6A (A), and MA-9 (B) in co-presence of 55 mM glucose and 5 mM vanillate. The data comprise mean values and deviations from three biological replicates.

low-cost value chain that avoids purification steps.

3.9. *C. glutamicum* MA-9 efficiently produces MA from structurally diverse aromatics, associated to different types of lignin

Besides the alkaline oxidization of softwood lignin that yields, predominantly, vanillin and vanillate, other chemical or microbial lignin depolymerization strategies lead to a range of further aromatic compounds, depending *inter alia* on the plant biomass, and the respective lignin type and monomeric composition (Bugg et al., 2011; Du et al., 2010; Lancefield et al., 2016; Pérez-Armada et al., 2019; Rodriguez et al., 2017; Wouter Schutyser et al., 2018a). These compounds include hydroxycinnamates, such as *p*-coumarate, ferulate, both derived from agricultural residues (Sun et al., 2002) and grasses (Yan et al., 2010), cereal-based caffeate (Hefni et al., 2019), but, also, other aromatic aldehydes (*p*-hydroxybenzaldehyde, protocatechualdehyde), major products from novel lignin degradation strategies (Dhar et al., 2020; Yang et al., 2019), and aromatic acids (*p*-hydroxybenzoate, protocatechuate), all metabolized *via* the protocatechuate branch of the β-ketoadipate pathway (Ding et al., 2015; Kallscheuer et al., 2016; Shen et al., 2012) (Fig. 1A). In a first inspection, we evaluated the capacity of the wildtype *C. glutamicum* to tolerate and assimilate these structurally diverse aromatic substrates, associated to H-, G-, and C-lignins (Vermaas et al., 2019), in the presence of glucose (Fig. 1, Fig. S1, Supplementary File 1).

Generally, *C. glutamicum* grew surprisingly well in the presence of all three hydroxycinnamates, given the fact that these aromatics were known for their pronounced antimicrobial activity (Lima et al., 2016; Lou et al., 2012). At higher concentrations of *p*-coumarate, ferulate, small amounts of the associated aromatic acids, vanillate and *p*-hydroxybenzoate, were detected, respectively (Fig. 1G). Regarding biomass formation (Fig. 1F) caffeate had the least inhibitory impact, partially related to its abiotic oxidation (Fig. S9, Supplementary File 1) (Vardon et al., 2015). Among the vanillin-analogues, *p*-hydroxybenzaldehyde significantly affected biomass formation, whereas *C. glutamicum* grew well up to concentrations of 10 mM protocatechualdehyde. Interestingly, *C. glutamicum* accumulated unknown hydrophilic metabolites, when grown on the two aldehydes (Fig. S2A, Fig. S2B, Supplementary File 1). Comparably to vanillin and vanillyl alcohol, they were identified as *p*-hydroxybenzyl alcohol and protocatechuyl alcohol (Fig. 1C), matching previous observations for related strains, including *C. glutamicum* S9114 (P. Zhou et al., 2019a) and *Rhodococcus opacus* PD630 (Zhou et al., 2022) that reduce differently substituted benzaldehydes into their benzyl alcohol derivatives. The fact, that the reduction of vanillin was much more pronounced compared to the reduction of *p*-hydroxybenzaldehyde and protocatechualdehyde (Fig. 1C), could likely explain, why vanillin was less toxic for *C. glutamicum* than the other aromatic aldehydes (Fig. 1B).

Among all tested substances, aromatic acids were found least inhibitory (Fig. 1D). Notably, *p*-hydroxybenzoate stimulated growth, and this effect was even more pronounced for protocatechuate (Fig. 1E). Curiously, protocatechuate was identified to be most toxic to *P. putida* among different aromatic compounds while similar concentrations of *p*-hydroxybenzoate increased the growth rates (Salvachúa et al., 2018), suggesting strain specific differences in the sensitivity to towards structurally similar aromatics that might come into play, when approaching different lignin-based streams (Lancefield et al., 2016; W. Schutyser et al., 2018b).

Next, we investigated the capability of different strains to produce MA from representative aromatic compounds with glucose as co-substrate (Fig. 8). *C. glutamicum* MA-6A, harboring the native *E. cloacae* gene cluster, produced MA from all tested aromatics (Fig. 8A). Notably, aromatic acids were completely converted into MA, whereas the efficiency to funnel aromatic aldehydes into MA was lower in general and revealed several metabolism-specific by-products.

Nicely, this natural deficiency in aromatic aldehyde metabolism was entirely overcome in our best producer *C. glutamicum* MA-9 (Fig. 8B), and, also, in *C. glutamicum* MA-7 (Fig. S10, Supplementary File 1). This suggested that in-line with the natural "biological funneling" (Linger et al., 2014) of aromatics *via* shared metabolic routes, the here-developed metabolic engineering strategy for enhanced vanillin assimilation also was favorable for enhanced aromatic aldehyde metabolism in more general terms.

In so-far, *C. glutamicum* MA-9 allowed by-product free MA-production from all tested aromatics, except for *p*-coumarate. The *p*-hydroxybenzoate accumulation, also apparent for strain MA-6A in *p*-hydroxybenzaldehyde-based cultivations, implied a bottleneck in PobA-functionality catalyzing the hydroxylation of *p*-hydroxybenzoate into protocatechuate, suggesting interesting synergies with previous engineering approaches in *P. putida* KT2440 (Johnson et al., 2016; Kuatsjah et al., 2022). Also, it appeared noteworthy, that strain MA-9 with enhanced *van*K expression grew faster on protocatechuate than strains MA-6A and MA-7 (Fig. 8, Fig. S10, Supplementary File 1).

All in all, MA-9 emerged as a highly robust and efficient cell factory to valorize structurally diverse aromatics into MA. As done before for other bacterial MA-producers (Cai et al., 2020; Kohlstedt et al., 2022; Salvachúa et al., 2018), the tolerance of the here-generated strain MA-9 against different aromatic substrates should be evaluated, which might also prove insightful regarding putative combinatorial toxicities of aromatic substrates and MA as a product (Salvachúa et al., 2018).

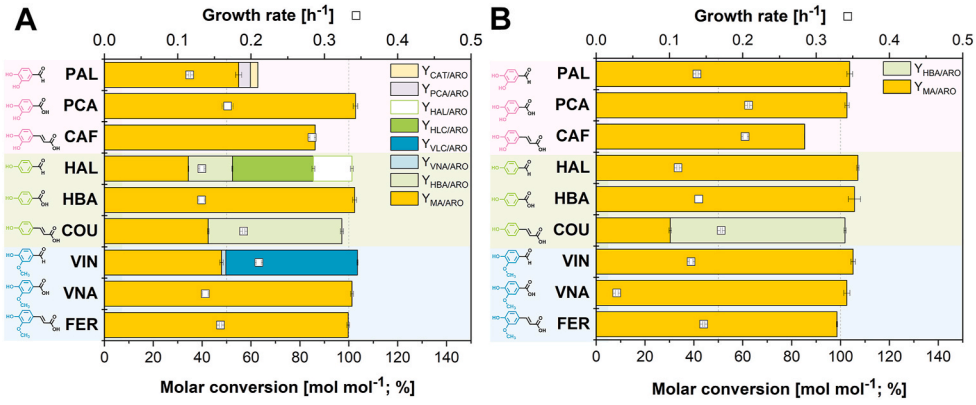

Fig. 8. Benchmarking *C. glutamicum* MA-6A (A) and MA-9 (B) for the valorization of nine structurally diverse lignin-associated aromatics. Both strains were cultivated in a microbioreactor supplying 5 mM of different aromatic aldehydes, acids, and hydroxycinnamates as biotransformation substrate for MA-production (blue, G-lignin substitution; green, H-lignin substitution; pink, C-lignin substitution) (Vermaas et al., 2019). Additionally, 55 mM glucose were provided as growth substrate. Strain performance was compared by end point measurements taken after 24 h. The data comprise mean values and deviations from three biological replicates. Abbreviations: CAF - caffeate, CAT - catechol, COU - *p*-coumarate, FER - ferulate, HBA - *p*-hydroxybenzoate, HAL - *p*-hydroxybenzaldehyde, HLC - *p*-hydroxybenzyl alcohol, MA - *cis, cis*-muconate, PAL - protocatechualdehyde, PCA - protocatechuate, VIN - vanillin, VLC - vanillyl alcohol, VNA - vanillate.

3.10. *FudC functions as a promiscuous aromatic aldehyde reductase in C. glutamicum*

Enzymes involved in aromatic degradation are often featured by substrate promiscuity allowing to degrade structurally similar compounds by analogous pathways (Weiland et al., 2022). Based on the discovery of aromatic alcohols being formed from *p*-hydroxybenzaldehyde and protocatechualdehyde, and the enhanced MA production performance for MA-7 and MA-9 from aromatic aldehydes, we hypothesized that, FudC shown to accept furfural (Tsuge et al., 2016) and vanillin (this work), could also convert these structurally similar aromatic aldehydes. Both the wildtype and the newly created *fudC* deletion mutant were grown on glucose plus protocatechualdehyde or *p*-hydroxybenzaldehyde, respectively (Fig. 9). For both aromatic aldehydes, the *fudC* deletion mutant did no longer produce the corresponding alcohols. FudC obviously functioned as an unspecific aromatic aldehyde reductase (Fig. S11, Supplementary File 1). Interestingly, in contrast to vanillyl alcohol, *p*-hydroxybenzyl alcohol (Fig. 9A) and protocatechuyl alcohol (Fig. 9C) were efficiently taken up again by *C. glutamicum* after formation. It seems likely that these two aromatic alcohols are processed through other metabolic routes in *C. glutamicum*, which remain to be investigated more closely in future studies. Indeed

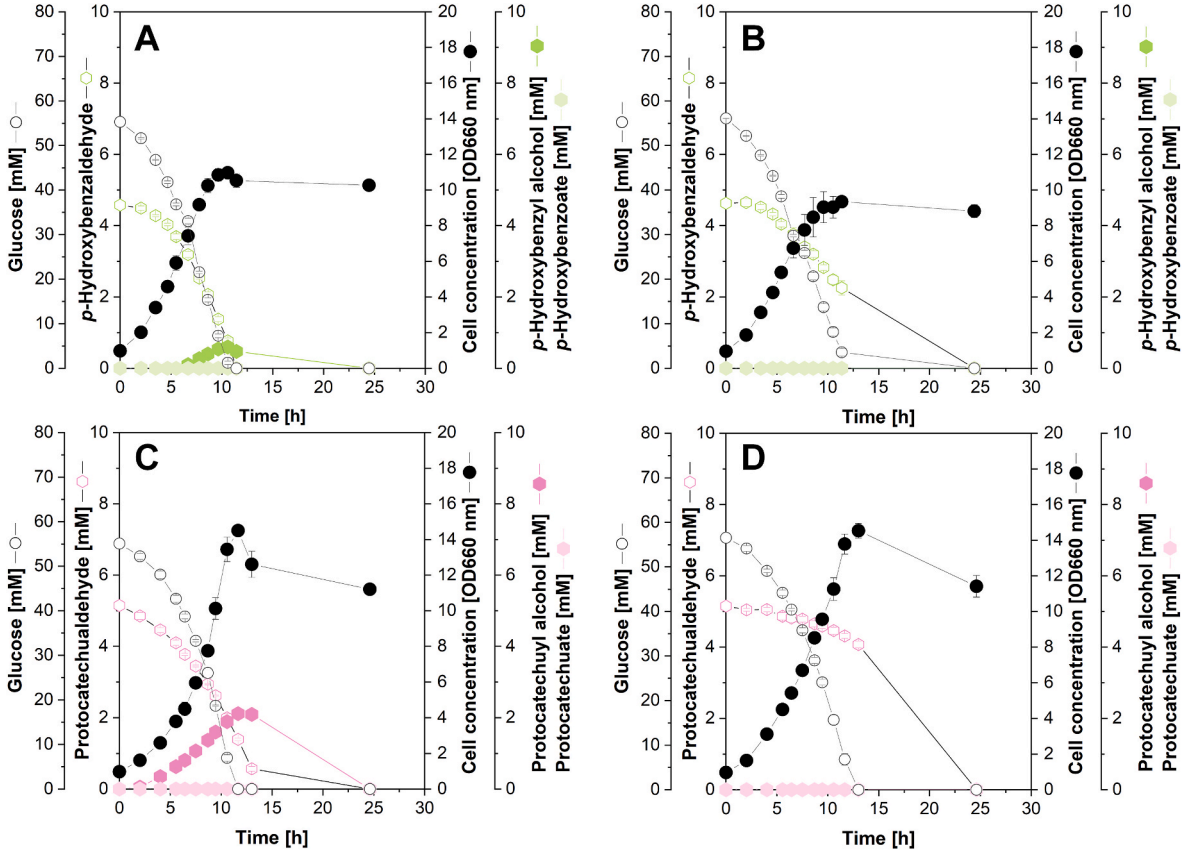

Fig. 9. Characterization of FudC as unspecific aromatic aldehyde reductase in *C. glutamicum*. Cultivation profiles of the wildtype (left) and the deletion mutant *ΔfudC* (right) on 55 mM glucose and 5 mM *p*-hydroxybenzaldehyde (A, B) or 5 mM protocatechualdehyde (C, D), respectively. For strain *ΔfudC* no aromatic alcohols were detected, suggesting that FudC has a promiscuous substrate spectrum. The data comprise mean values and deviations from three biological replicates.

p-hydroxybenzyl alcohol is a reported metabolic intermediate in *p*-cresol metabolism of *C. glutamicum* (Du et al., 2016), and, interestingly, protocatechuyl alcohol was considered as a putative intermediate in *p*-cresol metabolism of the fungus *Aspergillus fumigatus* (Jones et al., 1993).

4. Conclusions and outlook

As shown, systems metabolic engineering upgraded *C. glutamicum* to high-efficiency production of MA from various aromatics, including vanillin and vanillate. The two monomers are available at high yield through catalytic alkaline oxidation of softwood lignin (Wouter Schutyser et al., 2018a), a process that is established for a long-time at industrial scale (Pacek et al., 2013). Therefore, the created *C. glutamicum* cell factory MA-9 provides promising potential to valorize the massive streams of softwood lignin, heavily underutilized today. In this way, the established chemical conversion of bio-based MA to adipic acid (Vardon et al., 2015; Kohlstedt et al., 2018) and terephthalic acid (Kohlstedt et al., 2022) could direct industrially existing lignin streams to commercial plastics, such as nylon-6,6 (Kohlstedt et al., 2018) and PET (Kohlstedt et al., 2022), opening up a green and sustainable perspective for future manufacturing of these important products, unfavorably obtained from crude oil today. More work is needed to evaluate and further streamline the metabolically engineered microbe towards industrial applicability, including studies on internal process streams from alkaline-oxidized softwood lignin, which were not available here. Recently, the techno-economic assessment of MA production from aromatics out of lignin pyrolysis oil yielded a positive outcome in terms of energy and greenhouse gas savings and costs (van Duuren et al., 2020). We expect that MA production using vanillin- and vanillate-rich streams derived from oxidized lignin should yield a similar picture, but more work would be needed to quantitatively address this question, including precise specifications on the raw materials to be used. Clearly, only a very small fraction of potentially available lignin can be valorized into food-vanillin, given the small market size of the product, leaving substantial space for an MA-tailored industry.

From the raw material perspective, our development nicely complements previous efforts that demonstrated MA production from hydroxycinnamates towards lignin use from agricultural residues (Elmore et al., 2021; Rodriguez et al., 2017; Salvachúa et al., 2018) and, also, from phenolics, obtained from softwood and hardwood lignin through hydrothermal (Barton et al., 2018; Becker et al., 2018a; Kohlstedt et al., 2018) and pyrolytic depolymerization (van Duuren et al., 2020). In this regard, it provides a valuable extension to the aromatic substrate spectrum and accessible lignin streams. Hereby, the high natural robustness of *C. glutamicum* against the aromatic aldehyde vanillin, known as particularly toxic (Pattrick et al., 2019) and described as the major inhibitor in pre-treated lignocellulose (Chen et al., 2016), and its derivative vanillate, appeared as a valuable trait.

Beyond vanillin and vanillate, *C. glutamicum* MA-9 was also shown to efficiently handle a range of other, structurally diverse aromatics, namely caffeate, *p*-coumarate, ferulate, *p*-hydroxybenzoate, *p*-hydroxybenzaldehyde, protocatechualdehyde, and protocatechuate, suggesting broad application options and designating *C. glutamicum* as future platform host for lignin-based biotechnology, besides well-advanced and established microbes such as *P. putida* or *Rhodococcus* sp. (Bugg et al., 2021; Weiland et al., 2022). In this regard, our work provides an important proof-of-concept towards a future where the (mainly first generation) sugar-based product portfolio of *C. glutamicum*, including more than 70 value added compounds (Wolf et al., 2021) could be based on lignin in addition or even instead, although we are far away from that today and much work is ahead. Even more than that, we discovered that aromatic aldehydes are efficiently converted by *C. glutamicum* into the corresponding alcohols by the unspecific aromatic aldehyde reductase FudC, complementing recent findings on its impact for aromatic aldehyde production (Kim et al., 2022).

Notably, aromatic alcohols are interesting chemicals for bacterial production. Vanillyl alcohol serves as a flavoring agent, whereby conventional production suffers from low yield (Chen et al., 2017), whereas *p*-hydroxybenzyl alcohol is intensively studied for pharmaceutical and medical application (Choi et al., 2018; Kam et al., 2011; Kim et al., 2011). The here-gained insights in aromatic aldehyde metabolism in *C. glutamicum,* as well as the characterization of FudC as an aromatic aldehyde reductase, might open further opportunities to broaden the product portfolio from lignin-based aromatics.

Finally, an interesting result was the superiority of the native gene versions over the codon-adapted counterparts that were streamlined to the preferred codon usage of *C. glutamicum* (Fig. 5), similarly observed in a recent metabolic engineering study of *C. glutamicum* that reported native genes to outperform codon-optimized variants (Rohles et al., 2022). However in other cases, codon-optimization was found helpful to improve the expression of heterologous genes in the microbe (Kind et al., 2010; Milke et al., 2020). Here, the analysis of the relative adaptiveness of the tested AroY-variants to the codon usage of both the donor strains and *C. glutamicum* (https://gcua.schoedl.de/), suggested that the codon-optimization likely affected translational efficiency and protein folding (Liu, 2020; Samatova et al., 2021) (Fig. S6, Supplementary File 1). Overall, the success of codon-optimization is still difficult to predict (Webster et al., 2017) so that several potential donors and both types of codon-usage should be considered for metabolic engineering in order not to miss an optimum solution.

Author statement

Fabia Weiland, Nadja Barton, Michael Kohlstedt, Judith Becker: investigation, formal analysis; Fabia Weiland, Christoph Wittmann: visualization; Fabia Weiland, Christoph Wittmann: drafting and revising the manuscript; Fabia Weiland, Judith Becker, Christoph Wittmann: design of study, conceptualization; Christoph Wittmann: supervision, editing, resources, funding acquisition.

Declaration of competing interest

The authors have filed patent applications on the use of lignin for bio-production.

Data availability

Data will be made available on request.

Acknowledgements

All authors thanks Michel Fritz (Saarland University) for excellent support in analytics. Christoph Wittmann acknowledges support by the German Ministry for Education and Research (BMBF) through the grants LignoValue (FKZ 031B0344A) and MISSION (FKZ 031B0611A) and by the Leibniz-Science Campus Living Therapeutic Materials. Fabia Weiland thanks the HaVo Foundation, Ludwigshafen, Germany, for funding her through a doctoral fellowship. Judith Becker, Fabia Weiland, and Michael Kohlstedt acknowledge support through young investigator awards, sponsored by the Hans-and-Ruth-Giessen Foundation, St. Ingbert, Germany.

Appendix A. Supplementary data

Supplementary data to this article can be found online at https://doi.org/10.1016/j.ymben.2022.12.005.

References

Abdelaziz, O.Y., Brink, D.P., Prothmann, J., Ravi, K., Sun, M., García-Hidalgo, J., Sandahl, M., Hulteberg, C.P., Turner, C., Lidén, G., Gorwa-Grauslund, M.F., 2016.

Biological valorization of low molecular weight lignin. Biotechnol. Adv. 34, 1318–1346. https://doi.org/10.1016/j.biotechadv.2016.10.001.
Abu-Omar, M.M., Barta, K., Beckham, G.T., Luterbacher, J.S., Ralph, J., Rinaldi, R., Román-Leshkov, Y., Samec, J.S.M., Sels, B.F., Wang, F., 2021. Guidelines for performing lignin-first biorefining. Energy Environ. Sci. 14, 262–292. https://doi.org/10.1039/D0EE02870C.
Altschul, S., 1997. Gapped BLAST and PSI-BLAST: a new generation of protein database search programs. Nucleic Acids Res. 25, 3389–3402. https://doi.org/10.1093/nar/25.17.3389.
Altschul, S.F., Wootton, J.C., Gertz, E.M., Agarwala, R., Morgulis, A., Schaffer, A.A., Yu, Y.-K., 2005. Protein database searches using compositionally adjusted substitution matrices. FEBS J. 272, 5101–5109. https://doi.org/10.1111/j.1742-4658.2005.04945.x.
Barton, N., Horbal, L., Starck, S., Kohlstedt, M., Luzhetskyy, A., Wittmann, C., 2018. Enabling the valorization of guaiacol-based lignin: integrated chemical and biochemical production of *cis, cis*-muconic acid using metabolically engineered *Amycolatopsis* sp. ATCC 39116. Metab. Eng. 45, 200–210. https://doi.org/10.1016/j.ymben.2017.12.001.
Becker, J., Buschke, N., Bücker, R., Wittmann, C., 2010. Systems level engineering of *Corynebacterium glutamicum* - reprogramming translational efficiency for superior production. Eng. Life Sci. 10, 430–438. https://doi.org/10.1002/elsc.201000008.
Becker, J., Klopprogge, C., Zelder, O., Heinzle, E., Wittmann, C., 2005. Amplified expression of fructose 1,6-bisphosphatase in *Corynebacterium glutamicum* increases in vivo flux through the pentose phosphate pathway and lysine production on different carbon sources. Appl. Environ. Microbiol. 71, 8587–8596. https://doi.org/10.1128/AEM.71.12.8587-8596.2005.
Becker, J., Kuhl, M., Kohlstedt, M., Starck, S., Wittmann, C., 2018a. Metabolic engineering of *Corynebacterium glutamicum* for the production of *cis, cis*-muconic acid from lignin. Microb. Cell Factories 17, 115. https://doi.org/10.1186/s12934-018-0963-2.
Becker, J., Rohles, C.M., Wittmann, C., 2018b. Metabolically engineered *Corynebacterium glutamicum* for bio-based production of chemicals, fuels, materials, and healthcare products. Metab. Eng. 50, 122–141. https://doi.org/10.1016/j.ymben.2018.07.008.
Becker, J., Wittmann, C., 2019. A field of dreams: lignin valorization into chemicals, materials, fuels, and health-care products. Biotechnol. Adv. 37, 107360 https://doi.org/10.1016/j.biotechadv.2019.02.016.
Becker, J., Zelder, O., Häfner, S., Schröder, H., Wittmann, C., 2011. From zero to hero—design-based systems metabolic engineering of Corynebacterium glutamicum for l-lysine production. Metab. Eng. 13, 159–168. https://doi.org/10.1016/j.ymben.2011.01.003.
Bjørsvik, H.-R., Liguori, L., 2002. Organic processes to pharmaceutical chemicals based on fine chemicals from lignosulfonates. Org. Process Res. Dev. 6, 279–290. https://doi.org/10.1021/op010087o.
Bjørsvik, H.-R., Minisci, F., 1999. Fine chemicals from lignosulfonates. 1. Synthesis of vanillin by oxidation of lignosulfonates. Org. Process Res. Dev. 3, 330–340. https://doi.org/10.1021/op9900028.
Brink, D.P., Ravi, K., Lidén, G., Gorwa-Grauslund, M.F., 2019. Mapping the diversity of microbial lignin catabolism: experiences from the eLignin database. Appl. Microbiol. Biotechnol. 103, 3979–4002. https://doi.org/10.1007/s00253-019-09692-4.
Bruijnincx, P.C.A., Rinaldi, R., Weckhuysen, B.M., 2015. Unlocking the potential of a sleeping giant: lignins as sustainable raw materials for renewable fuels, chemicals and materials. Green Chem. 17, 4860–4861. https://doi.org/10.1039/C5GC90055G.
Bugg, T.D., Ahmad, M., Hardiman, E.M., Rahmanpour, R., 2011. Pathways for degradation of lignin in bacteria and fungi. Nat. Prod. Rep. 28, 1883. https://doi.org/10.1039/c1np00042j.
Bugg, T.D.H., Williamson, J.J., Alberti, F., 2021. Microbial hosts for metabolic engineering of lignin bioconversion to renewable chemicals. Renew. Sustain. Energy Rev. 152, 111674 https://doi.org/10.1016/j.rser.2021.111674.
Cai, C., Xu, Z., Xu, M., Cai, M., Jin, M., 2020. Development of a *Rhodococcus opacus* cell factory for valorizing lignin to muconate. ACS Sustain. Chem. Eng. 8, 2016–2031. https://doi.org/10.1021/acssuschemeng.9b06571.
Chaudhry, M.T., Huang, Y., Shen, X.-H., Poetsch, A., Jiang, C.-Y., Liu, S.-J., 2007. Genome-wide investigation of aromatic acid transporters in *Corynebacterium glutamicum*. Microbiology 153, 857–865. https://doi.org/10.1099/mic.0.2006/002501-0.
Chen, C., Pan, J., Yang, X., Guo, C., Ding, W., Si, M., Zhang, Y., Shen, X., Wang, Y., 2016. Global transcriptomic analysis of the response of *Corynebacterium glutamicum* to vanillin. PLoS One 11, e0164955. https://doi.org/10.1371/journal.pone.0164955.
Chen, Z., Shen, X., Wang, Jian, Wang, Jia, Zhang, R., Rey, J.F., Yuan, Q., Yan, Y., 2017. Establishing an artificial pathway for *de novo* biosynthesis of vanillyl alcohol in *Escherichia coli*. ACS Synth. Biol. 6, 1784–1792. https://doi.org/10.1021/acssynbio.7b00129.
Choi, J., Yeo, S., Kim, M., Lee, H., Kim, S., 2018. *p* -Hydroxybenzyl alcohol inhibits four obesity-related enzymes in vitro. J. Biochem. Mol. Toxicol. 32, e22223 https://doi.org/10.1002/jbt.22223.
D'Argenio, D.A., Segura, A., Coco, W.M., Bünz, P.V., Ornston, L.N., 1999. The physiological contribution of *Acinetobacter* PcaK, a transport system that acts upon protocatechuate, can Be masked by the overlapping specificity of VanK. J. Bacteriol. 181, 3505–3515. https://doi.org/10.1128/JB.181.11.3505-3515.1999.
del Río, J.C., Rencoret, J., Gutiérrez, A., Elder, T., Kim, H., Ralph, J., 2020. Lignin monomers from beyond the canonical monolignol biosynthetic pathway: another brick in the wall. ACS Sustain. Chem. Eng. 8, 4997–5012. https://doi.org/10.1021/acssuschemeng.0c01109.
Dhar, P., Teja, V., Vinu, R., 2020. Sonophotocatalytic degradation of lignin: production of valuable chemicals and kinetic analysis. J. Environ. Chem. Eng. 8, 104286 https://doi.org/10.1016/j.jece.2020.104286.
Ding, W., Si, M., Zhang, W., Zhang, Y., Chen, C., Zhang, L., Lu, Z., Chen, S., Shen, X., 2015. Functional characterization of a vanillin dehydrogenase in *Corynebacterium glutamicum*. Sci. Rep. 5, 8044. https://doi.org/10.1038/srep08044.
Draths, K.M., Frost, J.W., 1994. Environmentally compatible synthesis of adipic acid from D-glucose. J. Am. Chem. Soc. 116, 399–400. https://doi.org/10.1021/ja00080a057.
Du, B., Sharma, L.N., Becker, C., Chen, S.-F., Mowery, R.A., van Walsum, G.P., Chambliss, C.K., 2010. Effect of varying feedstock-pretreatment chemistry combinations on the formation and accumulation of potentially inhibitory degradation products in biomass hydrolysates. Biotechnol. Bioeng. 107, 430–440. https://doi.org/10.1002/bit.22829.
Du, L., Ma, L., Qi, F., Zheng, X., Jiang, C., Li, A., Wan, X., Liu, S.-J., Li, S., 2016. Characterization of a unique pathway for 4-cresol catabolism initiated by phosphorylation in *Corynebacterium glutamicum*. J. Biol. Chem. 291, 6583–6594. https://doi.org/10.1074/jbc.M115.695320.
Elmore, J.R., Dexter, G.N., Salvachúa, D., Martinez-Baird, J., Hatmaker, E.A., Huenemann, J.D., Klingeman, D.M., Peabody, G.L., Peterson, D.J., Singer, C., Beckham, G.T., Guss, A.M., 2021. Production of itaconic acid from alkali pretreated lignin by dynamic two stage bioconversion. Nat. Commun. 12, 2261. https://doi.org/10.1038/s41467-021-22556-8.
Erickson, E., Bleem, A., Kuatsjah, E., Werner, A.Z., DuBois, J.L., McGeehan, J.E., Eltis, L. D., Beckham, G.T., 2022. Critical enzyme reactions in aromatic catabolism for microbial lignin conversion. Nat. Catal. 5, 86–98. https://doi.org/10.1038/s41929-022-00747-w.
Fache, M., Boutevin, B., Caillol, S., 2016. Vanillin production from lignin and its use as a renewable chemical. ACS Sustain. Chem. Eng. 4, 35–46. https://doi.org/10.1021/acssuschemeng.5b01344.
Fleige, C., Meyer, F., Steinbüchel, A., 2016. Metabolic engineering of the actinomycete *Amycolatopsis* sp. strain ATCC 39116 towards enhanced production of natural vanillin. Appl. Environ. Microbiol. 82, 3410–3419. https://doi.org/10.1128/AEM.00802-16.
García-Hidalgo, J., Brink, D.P., Ravi, K., Paul, C.J., Lidén, G., Gorwa-Grauslund, M.F., 2020. Vanillin Production in *Pseudomonas* : whole-Genome sequencing of *Pseudomonas* sp. strain 9.1 and reannotation of *Pseudomonas putida* CalA as a vanillin reductase. Appl. Environ. Microbiol. 86 https://doi.org/10.1128/AEM.02442-19.
Gómez-Álvarez, H., Iturbe, P., Rivero-Buceta, V., Mines, P., Bugg, T.D.H., Nogales, J., Díaz, E., 2022. Bioconversion of lignin-derived aromatics into the building block pyridine 2,4-dicarboxylic acid by engineering recombinant *Pseudomonas putida* strains. Bioresour. Technol. 346, 126638 https://doi.org/10.1016/j.biortech.2021.126638.
Gonçalves, C.C., Bruce, T., Silva, C. de O.G., Fillho, E.X.F., Noronha, E.F., Carlquist, M., Parachin, N.S., 2020. Bioprospecting microbial diversity for lignin valorization: dry and wet screening methods. Front. Microbiol. 11, 1081. https://doi.org/10.3389/fmicb.2020.01081.
Hansen, E.H., Møller, B.L., Kock, G.R., Bünner, C.M., Kristensen, C., Jensen, O.R., Okkels, F.T., Olsen, C.E., Motawia, M.S., Hansen, J., 2009. De novo biosynthesis of vanillin in fission yeast (*Schizosaccharomyces pombe*) and baker's yeast (*Saccharomyces cerevisiae*). Appl. Environ. Microbiol. 75, 2765–2774. https://doi.org/10.1128/AEM.02681-08.
He, Z., Wiegel, J., 1996. Purification and characterization of an oxygen-sensitive, reversible 3,4-dihydroxybenzoate decarboxylase from *Clostridium hydroxybenzoicum*. J. Bacteriol. 178, 3539–3543. https://doi.org/10.1128/jb.178.12.3539-3543.1996.
Hefni, M.E., Amann, L.S., Witthöft, C.M., 2019. A HPLC-UV method for the quantification of phenolic acids in cereals. Food Anal. Methods 12, 2802–2812. https://doi.org/10.1007/s12161-019-01637-x.
Hirano, Y., Izawa, A., Hosoya, T., Miyafuji, H., 2022. Degradation mechanism of a lignin model compound during alkaline aerobic oxidation: formation of the vanillin precursor from the β-O-4 middle unit of softwood lignin. React. Chem. Eng. 7, 1603–1616. https://doi.org/10.1039/D2RE00036A.
Hoffmann, S.L., Jungmann, L., Schiefelbein, S., Peyriga, L., Cahoreau, E., Portais, J.-C., Becker, J., Wittmann, C., 2018. Lysine production from the sugar alcohol mannitol: design of the cell factory Corynebacterium glutamicum SEA-3 through integrated analysis and engineering of metabolic pathway fluxes. Metab. Eng. 47, 475–487. https://doi.org/10.1016/j.ymben.2018.04.019.
Huang, Y., Zhao, K., Shen, X.-H., Jiang, C.-Y., Liu, S.-J., 2008. Genetic and biochemical characterization of a 4-hydroxybenzoate hydroxylase from *Corynebacterium glutamicum*. Appl. Microbiol. Biotechnol. 78, 75–83. https://doi.org/10.1007/s00253-007-1286-0.
Johnson, C.W., Salvachúa, D., Khanna, P., Smith, H., Peterson, D.J., Beckham, G.T., 2016. Enhancing muconic acid production from glucose and lignin-derived aromatic compounds *via* increased protocatechuate decarboxylase activity. Metab. Eng. Commun. 3, 111–119. https://doi.org/10.1016/j.meteno.2016.04.002.
Jones, K.H., Trudgill, P.W., Hopper, D.J., 1993. Metabolism of *p*-cresol by the fungus *Aspergillus fumigatus*. Appl. Environ. Microbiol. 59, 1125–1130. https://doi.org/10.1128/aem.59.4.1125-1130.1993.
Kallscheuer, N., Vogt, M., Kappelmann, J., Krumbach, K., Noack, S., Bott, M., Marienhagen, J., 2016. Identification of the *phd* gene cluster responsible for phenylpropanoid utilization in *Corynebacterium glutamicum*. Appl. Microbiol. Biotechnol. 100, 1871–1881. https://doi.org/10.1007/s00253-015-7165-1.
Kam, K.-Y., Yu, S.J., Jeong, N., Hong, J.H., Jalin, A.M.A.A., Lee, S., Choi, Y.W., Lee, C.K., Kang, S.G., 2011. p-hydroxybenzyl alcohol prevents brain injury and behavioral impairment by activating Nrf2, PDI, and neurotrophic factor genes in a rat model of brain ischemia. Mol. Cell 31, 209–215. https://doi.org/10.1007/s10059-011-0028-4.

Khalil, I., Quintens, G., Junkers, T., Dusselier, M., 2020. Muconic acid isomers as platform chemicals and monomers in the biobased economy. Green Chem. 22, 1517–1541. https://doi.org/10.1039/C9GC04161C.

Kienberger, M., Maitz, S., Pichler, T., Demmelmayer, P., 2021. Systematic review on isolation processes for technical lignin. Processes 9, 804. https://doi.org/10.3390/pr9050804.

Kim, H.-S., Choi, J.-A., Kim, B.-Y., Ferrer, L., Choi, J.-M., Wendisch, V.F., Lee, J.-H., 2022. Engineered *Corynebacterium glutamicum* as the platform for the production of aromatic aldehydes. Front. Bioeng. Biotechnol. 10, 880277 https://doi.org/10.3389/fbioe.2022.880277.

Kim, S., Park, H., Song, Y., Hong, D., Kim, O., Jo, E., Khang, G., Lee, D., 2011. Reduction of oxidative stress by p-hydroxybenzyl alcohol-containing biodegradable polyoxalate nanoparticulate antioxidant. Biomaterials 32, 3021–3029. https://doi.org/10.1016/j.biomaterials.2010.11.033.

Kind, S., Jeong, W.K., Schröder, H., Wittmann, C., 2010. Systems-wide metabolic pathway engineering in Corynebacterium glutamicum for bio-based production of diaminopentane. Metab. Eng. 12, 341–351. https://doi.org/10.1016/j.ymben.2010.03.005.

Kohlstedt, M., Starck, S., Barton, N., Stolzenberger, J., Selzer, M., Mehlmann, K., Schneider, R., Pleissner, D., Rinkel, J., Dickschat, J.S., Venus, J., B.J.H. van Duuren, J., Wittmann, C., 2018. From lignin to nylon: cascaded chemical and biochemical conversion using metabolically engineered *Pseudomonas putida*. Metab. Eng. 47, 279–293. https://doi.org/10.1016/j.ymben.2018.03.003.

Kohlstedt, M., Weimer, A., Weiland, F., Stolzenberger, J., Selzer, M., Sanz, M., Kramps, L., Wittmann, C., 2022. Biobased PET from lignin using an engineered *cis, cis*-muconate-producing *Pseudomonas putida* strain with superior robustness, energy and redox properties. Metab. Eng. 72, 337–352. https://doi.org/10.1016/j.ymben.2022.05.001.

Korneli, C., Biedendieck, R., David, F., Jahn, D., Wittmann, C., 2013. High yield production of extracellular recombinant levansucrase by *Bacillus megaterium*. Appl. Microbiol. Biotechnol. 97, 3343–3353. https://doi.org/10.1007/s00253-012-4567-1.

Kuatsjah, E., Johnson, C.W., Salvachúa, D., Werner, A.Z., Zahn, M., Szostkiewicz, C.J., Singer, C.A., Dominick, G., Okekeogbu, I., Haugen, S.J., Woodworth, S.P., Ramirez, K.J., Giannone, R.J., Hettich, R.L., McGeehan, J.E., Beckham, G.T., 2022. Debottlenecking 4-hydroxybenzoate hydroxylation in Pseudomonas putida KT2440 improves muconate productivity from p-coumarate. Metab. Eng. 70, 31–42. https://doi.org/10.1016/j.ymben.2021.12.010.

Lancefield, C.S., Rashid, G.M.M., Bouxin, F., Wasak, A., Tu, W.-C., Hallett, J., Zein, S., Rodríguez, J., Jackson, S.D., Westwood, N.J., Bugg, T.D.H., 2016. Investigation of the chemocatalytic and biocatalytic valorization of a range of different lignin preparations: the importance of β-O-4 content. ACS Sustain. Chem. Eng. 4, 6921–6930. https://doi.org/10.1021/acssuschemeng.6b01855.

Leavitt, J.M., Wagner, J.M., Tu, C.C., Tong, A., Liu, Y., Alper, H.S., 2017. Biosensor-enabled directed evolution to improve muconic acid production in *Saccharomyces cerevisiae*. Biotechnol. J. 12, 1600687 https://doi.org/10.1002/biot.201600687.

Lee, H.-N., Shin, W.-S., Seo, S.-Y., Choi, S.-S., Song, J., Kim, J., Park, J.-H., Lee, D., Kim, S.Y., Lee, S.J., Chun, G.-T., Kim, E.-S., 2018. *Corynebacterium* cell factory design and culture process optimization for muconic acid biosynthesis. Sci. Rep. 8, 18041 https://doi.org/10.1038/s41598-018-36320-4.

Lima, V.N., Oliveira-Tintino, C.D.M., Santos, E.S., Morais, L.P., Tintino, S.R., Freitas, T.S., Geraldo, Y.S., Pereira, R.L.S., Cruz, R.P., Menezes, I.R.A., Coutinho, H.D.M., 2016. Antimicrobial and enhancement of the antibiotic activity by phenolic compounds: gallic acid, caffeic acid and pyrogallol. Microb. Pathog. 99, 56–61. https://doi.org/10.1016/j.micpath.2016.08.004.

Linger, J.G., Vardon, D.R., Guarnieri, M.T., Karp, E.M., Hunsinger, G.B., Franden, M.A., Johnson, C.W., Chupka, G., Strathmann, T.J., Pienkos, P.T., Beckham, G.T., 2014. Lignin valorization through integrated biological funneling and chemical catalysis. Proc. Natl. Acad. Sci. USA 111, 12013–12018. https://doi.org/10.1073/pnas.1410657111.

Liu, Y., 2020. A code within the genetic code: codon usage regulates co-translational protein folding. Cell Commun. Signal. 18, 145. https://doi.org/10.1186/s12964-020-00642-6.

Lou, Z., Wang, H., Rao, S., Sun, J., Ma, C., Li, J., 2012. *p*-Coumaric acid kills bacteria through dual damage mechanisms. Food Control 25, 550–554. https://doi.org/10.1016/j.foodcont.2011.11.022.

Merkens, H., Beckers, G., Wirtz, A., Burkovski, A., 2005. Vanillate metabolism in *Corynebacterium glutamicum*. Curr. Microbiol. 51, 59–65. https://doi.org/10.1007/s00284-005-4531-8.

Meyer, F., Netzer, J., Meinert, C., Voigt, B., Riedel, K., Steinbüchel, A., 2018. A proteomic analysis of ferulic acid metabolism in *Amycolatopsis* sp. ATCC 39116. Appl. Microbiol. Biotechnol. 102, 6119–6142. https://doi.org/10.1007/s00253-018-9061-y.

Milke, L., Mutz, M., Marienhagen, J., 2020. Synthesis of the character impact compound raspberry ketone and additional flavoring phenylbutanoids of biotechnological interest with Corynebacterium glutamicum. Microb. Cell Factories 19, 92. https://doi.org/10.1186/s12934-020-01351-y.

Morabbi Heravi, K., Lange, J., Watzlawick, H., Kalinowski, J., Altenbuchner, J., 2015. Transcriptional regulation of the vanillate utilization genes (*vanABK* operon) of *Corynebacterium glutamicum* by VanR, a PadR-Like Repressor. J. Bacteriol. 197, 959–972. https://doi.org/10.1128/JB.02431-14.

Mori, K., Kamimura, N., Masai, E., 2018. Identification of the protocatechuate transporter gene in *Sphingobium* sp. strain SYK-6 and effects of overexpression on production of a value-added metabolite. Appl. Microbiol. Biotechnol. 102, 4807–4816. https://doi.org/10.1007/s00253-018-8988-3.

Pacek, A.W., Ding, P., Garrett, M., Sheldrake, G., Nienow, A.W., 2013. Catalytic conversion of sodium lignosulfonate to vanillin: engineering aspects. Part 1. Effects of processing conditions on vanillin yield and selectivity. Ind. Eng. Chem. Res. 52, 8361–8372. https://doi.org/10.1021/ie4007744.

Pattrick, C.A., Webb, J.P., Green, J., Chaudhuri, R.R., Collins, M.O., Kelly, D.J., 2019. Proteomic profiling, transcription factor modeling, and genomics of evolved tolerant strains elucidate mechanisms of vanillin toxicity in Escherichia coli. mSystems 4, e00163. https://doi.org/10.1128/mSystems.00163-19, 19.

Payer, S.E., Marshall, S.A., Bärland, N., Sheng, X., Reiter, T., Dordic, A., Steinkellner, G., Wuensch, C., Kaltwasser, S., Fisher, K., Rigby, S.E.J., Macheroux, P., Vonck, J., Gruber, K., Faber, K., Himo, F., Leys, D., Pavkov-Keller, T., Glueck, S.M., 2017. Regioselective *para* -Carboxylation of Catechols with a Prenylated Flavin Dependent Decarboxylase. Angew. Chem. Int. Ed. 56, 13893–13897. https://doi.org/10.1002/anie.201708091.

Pérez-Armada, L., Rivas, S., González, B., Moure, A., 2019. Extraction of phenolic compounds from hazelnut shells by green processes. J. Food Eng. 255, 1–8. https://doi.org/10.1016/j.jfoodeng.2019.03.008.

Priefert, H., Rabenhorst, J., Steinbüchel, A., 2001. Biotechnological production of vanillin. Appl. Microbiol. Biotechnol. 56, 296–314. https://doi.org/10.1007/s002530100687.

Ravi, K., García-Hidalgo, J., Nöbel, M., Gorwa-Grauslund, M.F., Lidén, G., 2018. Biological conversion of aromatic monolignol compounds by a *Pseudomonas* isolate from sediments of the Baltic Sea. Amb. Express 8, 32. https://doi.org/10.1186/s13568-018-0563-x.

Rodriguez, A., Salvachúa, D., Katahira, R., Black, B.A., Cleveland, N.S., Reed, M., Smith, H., Baidoo, E.E.K., Keasling, J.D., Simmons, B.A., Beckham, G.T., Gladden, J. M., 2017. Base-catalyzed depolymerization of solid lignin-rich streams enables microbial conversion. ACS Sustain. Chem. Eng. 5, 8171–8180. https://doi.org/10.1021/acssuschemeng.7b01818.

Rødsrud, G., 2018. Borregaards transformation from a traditional P&P company to the worlds most advanced biorefinery. In: Workshop on the Non-binding Guidance on Cascading Use of. Woody) Biomass.

Rohles, C., Pauli, S., Gießelmann, G., Kohlstedt, M., Becker, J., Wittmann, C., 2022. Systems metabolic engineering of Corynebacterium glutamicum eliminates all by-products for selective and high-yield production of the platform chemical 5-aminovalerate. Metab. Eng. 73, 168–181. https://doi.org/10.1016/j.ymben.2022.07.005.

Rohles, C.M., Gießelmann, G., Kohlstedt, M., Wittmann, C., Becker, J., 2016. Systems metabolic engineering of *Corynebacterium glutamicum* for the production of the carbon-5 platform chemicals 5-aminovalerate and glutarate. Microb. Cell Factories 15, 154. https://doi.org/10.1186/s12934-016-0553-0.

Rohles, C.M., Gläser, L., Kohlstedt, M., Gießelmann, G., Pearson, S., del Campo, A., Becker, J., Wittmann, C., 2018. A bio-based route to the carbon-5 chemical glutaric acid and to bionylon-6,5 using metabolically engineered *Corynebacterium glutamicum*. Green Chem. 20, 4662–4674. https://doi.org/10.1039/C8GC01901K.

Rorrer, N.A., Dorgan, J.R., Vardon, D.R., Martinez, C.R., Yang, Y., Beckham, G.T., 2016. Renewable unsaturated polyesters from muconic acid. ACS Sustain. Chem. Eng. 4, 6867–6876. https://doi.org/10.1021/acssuschemeng.6b01820.

Salvachúa, D., Johnson, C.W., Singer, C.A., Rohrer, H., Peterson, D.J., Black, B.A., Knapp, A., Beckham, G.T., 2018. Bioprocess development for muconic acid production from aromatic compounds and lignin. Green Chem. 20, 5007–5019. https://doi.org/10.1039/C8GC02519C.

Samatova, E., Daberger, J., Liutkute, M., Rodnina, M.V., 2021. Translational control by ribosome pausing in bacteria: how a non-uniform pace of translation affects protein production and folding. Front. Microbiol. 11, 619430 https://doi.org/10.3389/fmicb.2020.619430.

Schutyser, Wouter, Kruger, J.S., Robinson, A.M., Katahira, R., Brandner, D.G., Cleveland, N.S., Mittal, A., Peterson, D.J., Meilan, R., Román-Leshkov, Y., Beckham, G.T., 2018a. Revisiting alkaline aerobic lignin oxidation. Green Chem. 20, 3828–3844. https://doi.org/10.1039/C8GC00502H.

Schutyser, W., Renders, T., Van den Bosch, S., Koelewijn, S.-F., Beckham, G.T., Sels, B.F., 2018b. Chemicals from lignin: an interplay of lignocellulose fractionation, depolymerisation, and upgrading. Chem. Soc. Rev. 47, 852–908. https://doi.org/10.1039/C7CS00566K.

Shanks, B.H., Broadbelt, L.J., 2019. A robust strategy for sustainable organic chemicals utilizing bioprivileged molecules. ChemSusChem 12, 2970–2975. https://doi.org/10.1002/cssc.201900323.

Shen, X., Liu, S.-J., 2005. Key enzymes of the protocatechuate branch of the β-ketoadipate pathway for aromatic degradation in *Corynebacterium glutamicum*. Sci. China, Ser. A C 48, 241. https://doi.org/10.1360/062004-32.

Shen, X.-H., Zhou, N.-Y., Liu, S.-J., 2012. Degradation and assimilation of aromatic compounds by *Corynebacterium glutamicum*: another potential for applications for this bacterium? Appl. Microbiol. Biotechnol. 95, 77–89. https://doi.org/10.1007/s00253-012-4139-4.

Shimizu, M., Kobayashi, Y., Tanaka, H., Wariishi, H., 2005. Transportation mechanism for vanillin uptake through fungal plasma membrane. Appl. Microbiol. Biotechnol. 68, 673–679. https://doi.org/10.1007/s00253-005-1933-2.

Shinoda, E., Takahashi, K., Abe, N., Kamimura, N., Sonoki, T., Masai, E., 2019. Isolation of a novel platform bacterium for lignin valorization and its application in glucose-free *cis,cis*-muconate production. J. Ind. Microbiol. Biotechnol. 46, 1071–1080. https://doi.org/10.1007/s10295-019-02190-6.

Silva, E.A.B. da, Zabkova, M., Araújo, J.D., Cateto, C.A., Barreiro, M.F., Belgacem, M.N., Rodrigues, A.E., 2009. An integrated process to produce vanillin and lignin-based polyurethanes from Kraft lignin. Chem. Eng. Res. Des. 87, 1276–1292. https://doi.org/10.1016/j.cherd.2009.05.008.

Sonoki, T., Morooka, M., Sakamoto, K., Otsuka, Y., Nakamura, M., Jellison, J., Goodell, B., 2014. Enhancement of protocatechuate decarboxylase activity for the effective production of muconate from lignin-related aromatic compounds. J. Biotechnol. 192, 71–77. https://doi.org/10.1016/j.jbiotec.2014.10.027.

Sonoki, T., Takahashi, K., Sugita, H., Hatamura, M., Azuma, Y., Sato, T., Suzuki, S., Kamimura, N., Masai, E., 2018. Glucose-free *cis, cis*-muconic acid production via new metabolic designs corresponding to the heterogeneity of lignin. ACS Sustain. Chem. Eng. 6, 1256–1264. https://doi.org/10.1021/acssuschemeng.7b03597.

Sun, R., Sun, X.F., Wang, S.Q., Zhu, W., Wang, X.Y., 2002. Ester and ether linkages between hydroxycinnamic acids and lignins from wheat, rice, rye, and barley straws, maize stems, and fast-growing poplar wood. Ind. Crop. Prod. 15, 179–188. https://doi.org/10.1016/S0926-6690(01)00112-1.

Suzuki, Y., Otsuka, Y., Araki, T., Kamimura, N., Masai, E., Nakamura, M., Katayama, Y., 2021. Lignin valorization through efficient microbial production of β-ketoadipate from industrial black liquor. Bioresour. Technol. 337, 125489 https://doi.org/10.1016/j.biortech.2021.125489.

Tian, J.-H., Pourcher, A.-M., Bouchez, T., Gelhaye, E., Peu, P., 2014. Occurrence of lignin degradation genotypes and phenotypes among prokaryotes. Appl. Microbiol. Biotechnol. 98, 9527–9544. https://doi.org/10.1007/s00253-014-6142-4.

Tsuge, Y., Kudou, M., Kawaguchi, H., Ishii, J., Hasunuma, T., Kondo, A., 2016. FudC, a protein primarily responsible for furfural detoxification in *Corynebacterium glutamicum*. Appl. Microbiol. Biotechnol. 100, 2685–2692. https://doi.org/10.1007/s00253-015-7115-y.

Tuck, C.O., Perez, E., Horvath, I.T., Sheldon, R.A., Poliakoff, M., 2012. Valorization of biomass: deriving more value from waste. Science 337, 695–699. https://doi.org/10.1126/science.1218930.

van Duuren, J.B.J.H., Wild, P.J., Starck, S., Bradtmöller, C., Selzer, M., Mehlmann, K., Schneider, R., Kohlstedt, M., Poblete-Castro, I., Stolzenberger, J., Barton, N., Fritz, M., Scholl, S., Venus, J., Wittmann, C., 2020. Limited life cycle and cost assessment for the bioconversion of lignin-derived aromatics into adipic acid. Biotechnol. Bioeng. 117, 1381–1393. https://doi.org/10.1002/bit.27299.

Vardon, D.R., Franden, M.A., Johnson, C.W., Karp, E.M., Guarnieri, M.T., Linger, J.G., Salm, M.J., Strathmann, T.J., Beckham, G.T., 2015. Adipic acid production from lignin. Energy Environ. Sci. 8, 617–628. https://doi.org/10.1039/C4EE03230F.

Vermaas, J.V., Dixon, R.A., Chen, F., Mansfield, S.D., Boerjan, W., Ralph, J., Crowley, M. F., Beckham, G.T., 2019. Passive membrane transport of lignin-related compounds. Proc. Natl. Acad. Sci. USA 116, 23117–23123. https://doi.org/10.1073/pnas.1904643116.

Vu, T.T., Lim, Y.-I., Song, D., Hwang, K.-R., Kim, D.-K., 2021. Economic analysis of vanillin production from Kraft lignin using alkaline oxidation and regeneration. Biomass Convers. Biorefinery. https://doi.org/10.1007/s13399-020-01212-z.

Wada, A., Prates, É.T., Hirano, R., Werner, A.Z., Kamimura, N., Jacobson, D.A., Beckham, G.T., Masai, E., 2021. Characterization of aromatic acid/proton symporters in *Pseudomonas putida* KT2440 toward efficient microbial conversion of lignin-related aromatics. Metab. Eng. 64, 167–179. https://doi.org/10.1016/j.ymben.2021.01.013.

Weber, C., Brückner, C., Weinreb, S., Lehr, C., Essl, C., Boles, E., 2012. Biosynthesis of *cis, cis* -muconic acid and its aromatic precursors, catechol and protocatechuic acid, from renewable feedstocks by *Saccharomyces cerevisiae*. Appl. Environ. Microbiol. 78, 8421–8430. https://doi.org/10.1128/AEM.01983-12.

Webster, G.R., Teh, A.Y.-H., Ma, J.K.-C., 2017. Synthetic gene design-The rationale for codon optimization and implications for molecular pharming in plants: synthetic Gene Design. Biotechnol. Bioeng. 114, 492–502. https://doi.org/10.1002/bit.26183.

Weiland, F., Kohlstedt, M., Wittmann, C., 2022. Guiding stars to the field of dreams: metabolically engineered pathways and microbial platforms for a sustainable lignin-based industry. Metab. Eng. 71, 13–41. https://doi.org/10.1016/j.ymben.2021.11.011.

Wittmann, C., Hans, M., Heinzle, E., 2002. *In vivo* analysis of intracellular amino acid labelings by GC/MS. Analytical biochemistry, 2 (307), 379–382. https://doi.org/10.1016/S0003-2697(02)00030-1.

Wolf, S., Becker, J., Tsuge, Y., Kawaguchi, H., Kondo, A., Marienhagen, J., Bott, M., Wendisch, V.F., Wittmann, C., 2021. Advances in metabolic engineering of *Corynebacterium glutamicum* to produce high-value active ingredients for food, feed, human health, and well-being. Essays Biochem. 65, 197–212. https://doi.org/10.1042/EBC20200134.

Wu, W., Liu, F., Singh, S., 2018. Toward engineering *E. coli* with an autoregulatory system for lignin valorization. Proc. Natl. Acad. Sci. USA 115, 2970–2975. https://doi.org/10.1073/pnas.1720129115.

Xiao, X., Si, M., Yang, Z., Zhang, Y., Guan, J., Chaudhry, M.T., Wang, Y., Shen, X., 2015. Molecular characterization of a eukaryotic-like phenol hydroxylase from *Corynebacterium glutamicum*. J. Gen. Appl. Microbiol. 61, 99–107. https://doi.org/10.2323/jgam.61.99.

Xie, N.-Z., Liang, H., Huang, R.-B., Xu, P., 2014. Biotechnological production of muconic acid: current status and future prospects. Biotechnol. Adv. 32, 615–622. https://doi.org/10.1016/j.biotechadv.2014.04.001.

Yan, J., Hu, Z., Pu, Y., Charles Brummer, E., Ragauskas, A.J., 2010. Chemical compositions of four switchgrass populations. Biomass Bioenergy 34, 48–53. https://doi.org/10.1016/j.biombioe.2009.09.010.

Yang, Y., Song, W.-Y., Hur, H.-G., Kim, T.-Y., Ghatge, S., 2019. Thermoalkaliphilic laccase treatment for enhanced production of high-value benzaldehyde chemicals from lignin. Int. J. Biol. Macromol. 124, 200–208. https://doi.org/10.1016/j.ijbiomac.2018.11.144.

Zhou, H., Xu, Z., Cai, C., Li, J., Jin, M., 2022. Deciphering the metabolic distribution of vanillin in *Rhodococcus opacus* during lignin valorization. Bioresour. Technol. 347, 126348 https://doi.org/10.1016/j.biortech.2021.126348.

Zhou, P., Khushk, I., Gao, Q., Bao, J., 2019a. Tolerance and transcriptional analysis of *Corynebacterium glutamicum* on biotransformation of toxic furaldehyde and benzaldehyde inhibitory compounds. J. Ind. Microbiol. Biotechnol. 46, 951–963. https://doi.org/10.1007/s10295-019-02171-9.

Zhou, X., Brentzel, Z.J., Kraus, G.A., Keeling, P.L., Dumesic, J.A., Shanks, B.H., Broadbelt, L.J., 2019b. Computational framework for the identification of bioprivileged molecules. ACS Sustain. Chem. Eng. 7, 2414–2428. https://doi.org/10.1021/acssuschemeng.8b05275.